Artificial Neuro-Fuzzy Inference System (ANFIS) Based Speed Control of Separately Excited DC Motor for Load Torque Variations

Mekelle University

Ethiopian Institute of Technology-Mekelle (EiT-M)

School of Electrical and Computer Engineering (Industrial Control and Instrumentation Engineering chair)

A thesis submitted to the school of Electrical and Computer Engineering of Mekelle University in partial fulfillment of the requirements for the degree of Masters of Science in Control and Instrumentation Engineering

By: **Kibrom Zerau**

Advisor: **Tilahun Beyene (Assistant Professor)**

Co advisor: **Haylay Hishe (MSc.)**

June, 2025

MEKELLE, ETHIOPIA

Mekelle University

Ethiopian Institute of Technology-Mekelle (EiT-M)

School of Electrical and Computer Engineering

M.Sc. Program in Control and Instrumentation

Final Thesis Acceptance Approval Form

1. Name: **Kibrom Zerau Alemayo** **I.D. EITM/PR176067/12**
2. Thesis Title: **Artificial Neuro-Fuzzy Inference System (ANFIS) Based Speed Control of Separately Excited DC Motor for Load Torque Variations**.
3. This is to certify that **Mr. Kibrom Zerau** has incorporated all the comments forwarded to him by the external and internal examiners during the thesis defense held on 19/08/2025.

3.1. Mr. Kibrom Zerau (Student)	Signature	09/9/2025 Date
3.2. Mr. Tilahun Beyene (Advisor)	Signature	09/09/2025 Date
3.3 Dr. Zenachew Muluneh (Internal Examiner)	Signature	09/09/2025 Date
3.4 Dr. Chala Merga (External Examiner)	Signature	09/09/2025 Date
3.5. Mr. Hailay Hishe (Head, Industrial Control Engineering Chair)	Signature	09/09/2025 Date
3.6. Mr. Adhena Nigus (Head, School of ECE)	Signature	15/09/2025 Date

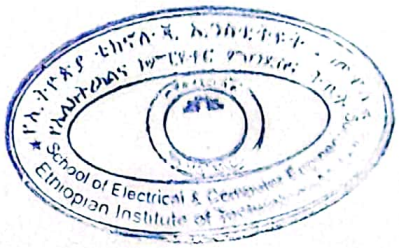

Acknowledgment

First and foremost, I would like to thank the almighty God for helping me to achieve my goal and to complete this thesis successfully. And then, I would like to thank Mekelle University for giving me the chance to study my master of degree and helping me financially.

I would like to express my sincere gratitude to my advisor Tilahun Beyene (Assistant Professor) for his persistent support, constant inspiration, valuable expert advice, suggestions and guidance throughout this thesis work.

My profound gratitude is extended to my co-advisor, Haylay Hishe (MSc.), His support, helpful criticism, and guidance were crucial in getting past obstacles during this study process and preparing me enough time schedule to finish the thesis work.

Abstract

Separately excited direct Motor (SEDCM) is an electromechanical actuator used to power different loads across several industrial and domestic applications. One fundamental characteristic for controlling when driving is the motor's speed. The external load linked to the drive negatively impacts speed if the controller is weak and the load varies. Objective of this thesis work is to design an Artificial Neuro-Fuzzy Inference System (ANFIS)-based speed control mechanism for a separately excited DC motor under varying load torque conditions. The ANFIS controller integrates neural networks and fuzzy logic to improve motor speed regulation, ensuring robust performance despite disturbances in load torque. Additionally, this this work explores the effectiveness of armature voltage control (source voltage adjustment) for dynamically regulating motor speed, comparing its performance with conventional control strategies. ANFIS, fuzzy logic controllers, PID controllers, and open loop (without controller) have all been used to measure the speed of an independently stimulated SEDC motor. At first, the motor speed can be regulated and modified by changing the armature voltage (the input supply voltage).When the torque of the load grows and the transient and steady state faults rise, the motor's speed falls in the absence of a controller. The motor performs poorly as a result, and its speed will not maintain its rated level. A PID controller improves the motor's speed over an open loop, but the overall performance is still poor and there are still some transient and steady state issues. Although fuzzy logic controllers perform better than PID controllers in terms of system performance, the speed still fluctuates as the torque of the load changes. However, ANFIS better than fuzzy, PID, and open loop control systems, operates at its rated speed, has low steady state and transient errors, and keeps the motor's speed constant as the load increases.

In conclusion, NFIS is superior to fuzzy and PID controllers due to its zero overshoot and reduced 38.31% settling time compared to fuzzy and 50.93 % compared to PID, reduced 37.12% rise time compared to fuzzy and 44.87 % compared to PID, and reduced 85% steady-state error compared to fuzzy and 98.5 % compared to PID. Additionally, by resolving the motor's nonlinear properties, the system's overall performance will improve.

Key word: ANFIS SEDCM, PID Controller, Fuzzy Controller,

Table of Contents

List of Figure

List of Table

List of Acronyms

FLC	Fuzzy Logic Controller
ANFIS	Artificial Neuro-Fuzzy Inference System
PWM	Pulse Width Modulation
PID	Proportional Integral Derivative
K_p	Proportional gain
K_D	Derivative gain
AC	Alternate current
DC	Direct current
ENL	Error negative large
ENS	Error negative small
EZ	Error zero
EPS	Error positive small
EPL	Error positive large
CENL	Change of error negative large
CENS	Change of error negative small
CEZ	Change of error zero
CEPS	Change of error positive small
CEPL	Change of error positive large
VS	Very small
S	Small
M	Medium
L	Large
VL	Very large
V_b	Back electromagnetic force (emf)
R_a	Armature resistance
L_a	Armature inductance
K_t	Damping friction of the mechanical system
K_e	Back electromotive force constant

$\mathbf{J_M}$	Moment of inertia of the rotor
$\mathbf{T_M}$	Torque of motor
W	Angular velocity
$\mathbf{T_L}$	Load torque
$\mathbf{B_M}$	Friction coefficient

CHAPTER ONE
INTRODUCTION

1.1. Background

The DC motor is a valuable device in many industrial uses that require changeable speed and load characteristics due to its ease of control; moreover, DC motor systems are essential for modern businesses. DC motors are employed in many different uses within industrial electronics and robotics, encompassing precision positioning and speed regulation. The regulation of speed of a DC motor is essential in applications where accuracy and safeguarding are essential. The DC motor has excellent speed control responsiveness and is extensively utilized in speed control systems that demand high precision, include rolling mills and double-hulled tankers, and high-precision digital equipment [1,2].

DC drives exhibit reduced complexity due to a singular power conversion process from AC to DC. The speed-torque characteristics of DC motors are significantly superior to those of AC motors. DC motors offer superior speed control for both acceleration and deceleration. DC drives are often more economical for the majority of horsepower levels. DC motors possess an extensive history as adjustable speed devices, and an extensive range of choices has developed for this function. In these applications, the motor must be properly regulated to get the necessary performance [3]**.**

The speed of DC motors can be changed across extensive ranges, facilitating enhanced controllability and superior performance. The speed control of DC motors was first implemented by voltage regulation by Ward Leonard in 1981 [4]. The controlled voltage sources employed for DC motor speed control have become increasingly significant with the development of thyristors as switching devices in power electronics. Subsequently, semiconductor components such as MOSFETs, IGBTs, and GTOs have been utilized as electrical switching devices.[5].

Separately excited DC motors are typically utilized as motors in industrial applications. These motors possess the advantages of minimal friction, compact dimensions, enhanced speed, reduced manufacturing costs, and high torque. Mathematical modeling is a crucial and frequently challenging step in understanding the physical principles of a DC motor; an accurate model is essential for developing the motor equations and the transfer function that correlates the input and output data. Several properties of the DC motor are complex and can be identified through measurements. Therefore, we want parameter estimate methodologies [6].

DC motors use feedback controllers to manage speed, position, or both. The speed controllers designed to regulate The speed of DC motors for various tasks include several conventional and numerical types, including Proportional Integral (PI) and Proportional Integral Derivative (PID), Fuzzy Logic Controller (FLC), or combinations between them. Artificial Neuro-Fuzzy Inference System (ANFIS) [7]. The proportional-integral-derivative (PID) controller regulates the majority of control systems worldwide. Reports indicate that over 95% of controllers utilized in industrial process control applications are of the PID selection, as no alternative controller matches the simplicity, clarity of functionality, applicability, and simplicity of use provided by the PID controller. PID controllers deliver stable and reliable performance for most systems when the PID parameters are well tuned; nevertheless, they do not yield good results in circumstances requiring adaptive algorithms [8].

Fuzzy logic control (FLC) is a famous application of fuzzy set theory, proposed by L.A. Zadeh in 1973 and subsequently implemented by Mamdani in 1974 to manage systems that are architecturally challenging to represent. Since that time, FLC has grown as a highly active and productive research domain, with numerous documented industrial applications [9]. Over the past thirty years, FLC has developed as a substitute or supplement to traditional control systems in multiple engineering domains. Fuzzy control theory typically offers non-linear controllers efficient at executing many sophisticated non-linear control actions, even in the presence of uncertain non-linear systems.

The Fuzzy Logic Controller provides several solutions. A fundamental advantage of a Fuzzy Logic Controller is that it doesn't require an extensive mathematical representation of the system. The popularity of FLC is attributed to its simple yet successful integration of human cognitive processes into its control mechanism. Fuzzy controllers exhibit robustness in the face of dynamic changes and have a broad stability range. FLC depends only on approximation and linguistic data [10]. The fundamental continuous feedback controller is the PID controller, which demonstrates outstanding performance. However, it is only sufficiently adaptive with flexible testing. Numerous sophisticated control strategies, including self-tuning control, model reference adaptive control, sliding mode control, and fuzzy logic control, have been developed to enhance system performance.

Neural Networks (NNs), also known as Artificial Neural Networks (ANNs), are computational systems modeled after the structure and functions of the human brain. An input layer acquires data,

one or more hidden layers analyze it, and an output layer produces a result. These models consist of interconnected nodes, or neurons, organized in layers. Each neuron possesses a bias, and each connection between neurons has an associated weight. In the training process, the network is presented with a dataset and systematically modifies its parameters to reduce the difference between its predictions and the actual outcomes. This enables the network to learn by adjusting these weights and biases [11].

The ability of neural networks (NNs) to uncover complex and non-linear relationships within data is one of their greatest strengths. This ability enables them to be utilized in a wide range of contexts. There are many different kinds of neural networks, and each one is designed to accomplish a specific type of task. There are two types of neural networks: recurrent neural networks (RNNs) and convolutional neural networks (CNNs). RNNs are particularly effective at processing sequential data, such as text and time series, while CNNs are particularly adept at interpreting pictures and videos. Following their remarkable performance in natural language processing, transformers, a different type, are increasingly being applied in a variety of other industries. These networks are crucial to the field of artificial intelligence in the modern era, since they make it possible to do tasks such as machine translation and medical diagnosis, as well as speech and image recognition [11,12].

The robust hybrid intelligence system named Adaptive Neuro-Fuzzy Inference System (ANFIS) effectively integrates the interpretability and human-like reasoning of fuzzy logic with the learning skills of artificial neural networks. ANFIS uses the Takagi-Sugeno fuzzy inference model to autonomously build or optimize fuzzy IF-THEN rules and their associated membership functions from data. Unlike the many nature of many pure neural networks, this synergy allows ANFIS to comprehend complex, non-linear interactions while preserving a degree of clarity in its decision-making process [13].

ANFIS design generally consists of five layers, each executing a distinct function in the fuzzy inference process, ranging from the fuzzification of inputs to the ultimate defuzzified output. ANFIS training utilizes a hybrid learning algorithm: a forward pass employs a least-squares method to optimize the consequent parameters, while a backward step use gradient descent to modify the antecedent parameters associated with the fuzzy membership functions. The adaptive characteristics of ANFIS allow it to effectively represent systems characterized by imprecision and

uncertainty, rendering it appropriate for control systems, forecasting, and pattern recognition, where both data-driven learning and rule-based interpretability are required [13].

1.2. Literature Review

Due to its wide application area, DC motor speed control is extensively studied by numerous authors, Some of the authors and their work is reviewed below.

J. Raheem Rashed (2019) [14] presented a simulation of speed control for a separately excited DC motor utilizing a fuzzy logic controller. In the work on speed control of separately excited DC motors through a fuzzy logic controller, he developed a technique that exceeds traditional controllers due to its superior performance and enhanced durability. A Fuzzy Logic Controller applied to a DC motor is examined. By employing suitable expert guidelines, there is no overshoot, minimal settling time, optimal rise time, and the steady-state error remains within the specified parameters. The primary limitation lies in the constant speed assumption, which fails to allow for variations in load torque.

(Hameed and Mohamad, 2012) [1] Presented on the speed control of a separately excited DC motor utilizing a fuzzy neural model reference controller. The research on speed control of a separately stimulated DC motor with a fuzzy neural model reference controller describes a technique that outperforms traditional controllers in terms of performance and endurance. The technology adaptively adjusts its fuzzy logic parameters through neural networks to follow a specified reference model, hence providing improved performance and resilience in nonlinear systems. This offers a substantial advantage over fixed-gain PID controllers and rule-based Fuzzy controllers by autonomously developing optimal control strategies. However, the variation in load torque was not taken into consideration.

(S. Bhowmik and A. Mitra, 2023) [15] Presented on the design of a PID controller for a separately excited DC motor and its performance analysis. The control system involving a PID controller for a DC motor was simulated in MATLAB. The performance and analysis of the DC motor with a PID controller was performed, calculating various responses of parameters such as maximum overshoot, rise time, and settling time, while excluding load torque and nonlinear effects such as friction and saturation.

(R. Nagarajan et al., 2017) [16] Presented on the implementation of chopper-fed speed control for a separately excited DC motor with a PI controller. The controller parameters were updated with the parameter alterations, and the Proportional Integral (PI) controller was utilized to adjust

the system response to the essential value, achieving stability by eliminating steady-state error rather than minimizing overshoot. evaluated exclusively under no-load conditions. The simulation results indicated that the system exhibited a rapid rise time, minimal settling time, and significant overshoot as the adaptation gains of the controller parameters were constantly raised.

(Khanke and Jain, 2015) [7] Presented controlling the speeds of a separately excited DC Motor employing multiple conventional controllers. Employing conventional controllers for controlling the speed of separately Excited DC Motors is popular. The study discusses various conventional controllers, including proportional (P), proportional-derivative (PD), proportional-integral (PI), and proportional-integral-derivative (PID). The results section of the report indicates that even with a linear load supplied to all controllers, their responses exhibited significant overshoot and delayed settling times. This thesis excludes variation load torque, unknown output disturbance signals, and nonlinear effects such as friction and saturation.

This thesis work addresses critical gaps identified in the control of Separately Excited DC (SEDC) motors. Conventional control methods often have difficulties maintaining consistent speed when confronted with varying load torques and the motor's natural nonlinear properties. These constraints typically result in undesirable performance, including slow response times, considerable speed overshoot and persistent steady-state errors. To address these issues, my thesis work proposes an Artificial Neuro-Fuzzy Inference System (ANFIS)-based control system. The new technique provides a more straightforward, quick, and dependable solution by using ANFIS's capacity to model and manage the motor's nonlinear behavior effectively. The suggested control system is specifically designed to provide a rapid reaction, thereby ensuring the desired speed regardless of load torque variations and also The resultant control system exhibits zero overshoot, little steady-state error, and quicker settling and rising times, all of which represent a substantial improvement over existing methods. This thesis work not only enhances the performance of SEDC motors but also provides a robust and efficient control solution for complex systems.

1.3. Statement of the Problem

DC motors are utilized in various applications, resulting in speed variations based on specific conditions. When a motor is designed to function at a constant speed, variations in load can lead to changes in its speed. Specifically, an increased load results in a reduction of the motor's speed, while a decreased load leads to an increase in the motor's speed. The motor operates inaccurately and does not function at its planned time. Machines can be easily damaged without the

implementation of a control methodology within their systems. The conventional techniques, including PI, PD, and PID, are extensively utilized in the control of speed and position for DC motors. The PID controller's low robustness makes it unsuitable for high-performance applications. The substantial obstacles in executing a traditional control system in a speed controller include the impact of the nonlinear characteristics of a DC motor, such as saturation and friction, which can adversely affect the performance of conventional controllers.

This thesis work proposed a new ability of the Artificial Neuro-Fuzzy Inference System (ANFIS). This approach provides a simpler, faster, and more dependable solution, which has distinct advantages over traditional Proportional-Integral-Derivative (PID) controllers and fuzzy logic systems. The proposed control system is designed to deliver a rapid response, ensuring that the speed of the DC motor is maintained at the desired level with zero overshoot, minimal steady-state error, and reduced settling time regardless of the variation of Load torque. Additionally, a quick rise time is essential and critical for industrial applications.

1.4. Objective

1.4.1. General Objective

The general objective of this thesis work is to Design an Artificial Neuro-Fuzzy Inference System (ANFIS) Based Speed Control of Separately Excited DC Motor for Load Torque Variations.

1.4.2. Specific Objective

To achieving the general objective**,** the following specific objectives have been accomplished in this thesis:

- ✓ Test the system performance without controller
- ✓ To analysis system performance under different load.
- ✓ To design buck Converter and analysis system performance
- ✓ Test and evaluate the system performance with PID, FUZZY and ANFIS using rise time, settling time, overshoot, and steady state error.
- ✓ Select the better controller for the system.

1.5. Scope of the Thesis

The scope of this thesis is to study, design, and simulate the speed control of the separately excited DC motor by Varying Load torque utilizing ANFIS exclusively through MATLAB/Simulink software. This study involves comparing the performance of the ANFIS controller with that of a fuzzy logic controller and a conventional PID controller, with results being observed through simulations conducted in MATLAB software, indicating that there will be no practical implementation.

1.6. Methodology

For the accomplishment of design Artificial Neuro-Fuzzy Inference System (ANFIS) Based Speed Control of Separately Excited DC Motor for Load Torque Variations, the following methodologies have been followed to achieve the specific objectives stated above.

- To study the gap and select proper controller, I have made review of recent related literature (articles, journals, published papers). And deal the basic Speed Control of Separately Excited DC Motor and mathematical model of the system (SEDC).
- System Modeling is conducted. Additionally, a mathematical model is presented, illustrating all the dynamics of the system along with the required steps.
- To design a PID controller. Traditionally, PID controllers are adjusted either through manual techniques or by employing rule-based approaches. Manual tuning methods require multiple iterations and can be quite time-intensive, while rule-based methods also present significant constraints. The automatic tuning of the PID controller is utilized to achieve optimal system design and fulfill design requirements.
- To develop a fuzzy logic controller. Creating a Fuzzy Logic Controller requires the development of fuzzy sets and IF-THEN rules for converting linguistic knowledge into an effective control strategy. The rules are afterwards processed by an inference engine and defuzzified to produce a precise control output.
- The ANFIS controller for speed control of SEDC has been designed, with training conducted using a conventional PID controller. The design of an Adaptive Neuro-Fuzzy Inference System (ANFIS) combines neural networks with fuzzy logic. Typically, input-output data is utilized for automatically changing the parameters of a fuzzy inference system. ANFIS possesses the capability to learn and adapt through a hybrid learning

process that often integrates backpropagation and least-squares methods. This enables the modeling of complex nonlinear relationships and produces results that are simple to understand.

- To measure, the effectiveness (performance) of the ANFIS controller for Speed Control of (SEDC) as compared with Fuzzy and PID Controller using MATLAB/ Simulink.

1.7. Organization of the Thesis

This study is systematically organized into five interconnected chapters including the introduction part. These are organized as follows:

• **Chapter Two**: Presents the theoretical overview of speed control of separately excited DC motor, types of DC motor, it also discusses the mathematical modeling of separately excited DC motor to easily doing the control system.

. Chapter Three: deals with the controller design i.e., describes Fuzzy inference system (FIS), types of membership function (MF), methods of fuzzy inference system, ANFIS controller, PID controller, hybrid learning and back propagation learning algorithm and designing Adaptive neuro-fuzzy inference system (ANFIS) for the proposed system.

. Chapter Four: briefs the result and discussion on the proposed controller and compare them with fuzzy logic and conventional (PID) controller. Finally, the performance of each controller is measured. Moreover, it presents the discussion about the performance of PID, fuzzy and ANFIS controller with variation of load torque.

. Chapter Five: draws the conclusions on the research and recommendation to future works.

CHAPTER TWO

Theoretical background and System modeling

2.1. Parts of DC Motor

DC motors are versatile and are frequently used in industrial applications. Diverse torque-speed characteristics can be achieved through various configurations of the field winding. A DC motor powers a mechanical load that transforms the provided electrical energy into mechanical energy. DC motors are increasingly being used, particularly in circumstances demanding substantial and precisely regulated torque. These motors are used in rolling mills, overhead cranes, and for traction applications such as forklift trucks, electric vehicles, and electric trains. They are utilized in portable machine tools powered by batteries, in automotive vehicles as starter motors and blower motors, and in other control applications as actuators [17].

DC motors have essentially three major parts:

A). Field system (stator) B). Armature (Rotor) and C). Commutator

The cut away view of DC motor parts are shown in Figure 2.1

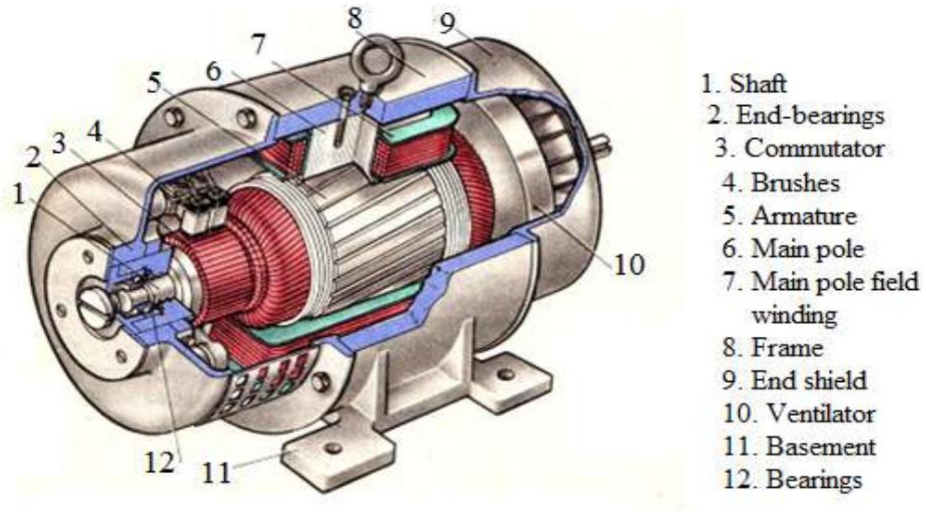

Figure 2.1: Cut away view of DC motor [17]

2.1.1. Field System

The field system sits on the stationary component of the motor known as the stator. The field system is intended for generating magnetic flux and, thus, supplies the requisite excitation for motor functioning. If the field is powered by an external DC source, the motor is referred to as a

separately excited DC motor; if the field is energized using armature voltage, it is termed a self-excited DC motor [17].

2.1.2. Armature

The armature is the rotor of the DC motor, where electromechanical energy conversion happens. The armature is a cylindrical structure that rotates between the magnetic poles.

The armature and the field system are separated from each other by an air gap. The armature consists of:

1. Armature core with slots and
2. Armature winding accommodated in slots

The armature's function is to rotate the conductors within a uniform magnetic field, therefore inducing an alternating electromotive force in its winding. The armature core is often constructed from high-permeability silicon-steel laminations with a thickness of 0.4 to 0.5 mm, isolated from each other by varnish or ceramic insulation [17].

2.1.3. Commutator

It is connected to the rotor of a DC motor and enables mechanical power rectification from DC to AC through the assistance of brushes in the case of motors. The terminals of the armature coils are linked to the commutator. It exhibits a cylindrical form and is situated at the ends of the armature. Brushes are required to conduct current to the DC motor via the that revolves commutator. Typically, brushes are composed of carbon and graphite to prevent damage to the commutator surface during contact. The brush is positioned in the brush holder, where a spring exerts pressure against the commutator [17].

A DC motor operates on the principle that a current-carrying conductor placed within a magnetic field experiences a mechanical force, resulting in the conductor's movement in the direction of the applied force. The magnitude of the mechanical force acting on the conductor is expressed as $F = Bia I$, where B denotes the magnetic field strength in Teslas (wb/m^2), ia represents the armature current in amperes, and I signifies the length of the conductor in meters. Upon connecting the motor to the DC supply mains, direct current flows through the brushes and commutator to the armature winding, generating torque by electromagnetic activities that facilitate rotor rotation.

The motor's inertia and friction, along with the mechanical load it drives, will generate a counter-clockwise torque that opposes the motor's rotation [17]. As the armature conductors rotate inside the magnetic field, electromotive force (emf) is induced in the armature conductors. The

orientation of the induced electromotive force, Eb, as ascertained by Fleming's right-hand rule, is directly contrary to the applied armature voltage. The induced electromotive force of a motor is commonly referred to as the back electromotive force (Eb). The applied voltage must be sufficiently high to surpass the back electromotive force and to drive the current through the armature's resistance. The electrical energy provided to counteract this resistance is transformed into mechanical energy in the armature.

2.2. Types of DC Motor

DC motors are classified into four types based on their excitation source: individually excited, shunt, series, and compound**.**

2.2.1. Separately Excited

As the name implies, an independently excited DC motor receives distinct power supplies for the field and armature windings. The primary distinguishing characteristic of these sorts of DC motors is that the armature current does not traverse the field winding, as the field winding is powered by a separate external source of DC current, as illustrated in figure 2.2 below.

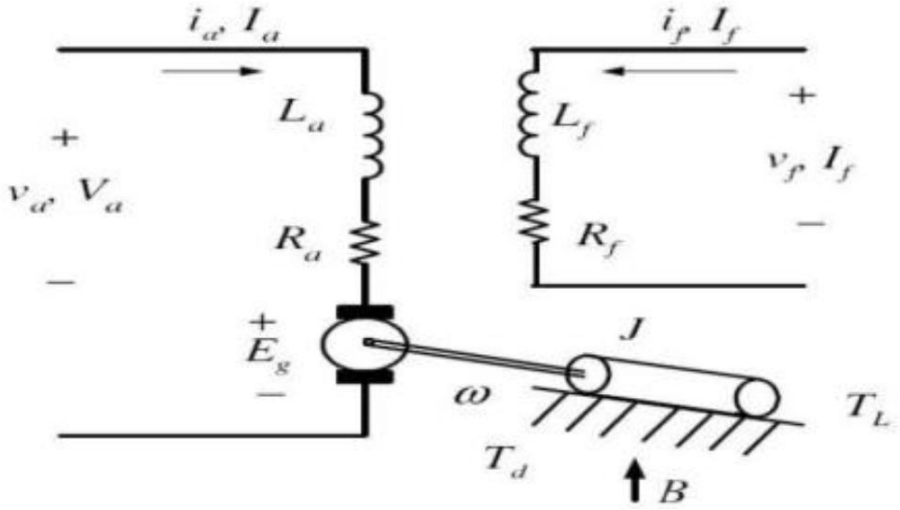

Figure 2.2: Circuit of separately excited DC motor [7]

The primary advantages of this type of motor include its effectiveness in variable speed control, as the field can be connected to a constant voltage while the armature can be linked to a variable DC source for speed regulation. Additionally, the motor facilitates reversal by simply reversing the polarity of the field supply, enabling operation in the reverse direction [7].

This motor is suitable for applications demanding speed variations from low to high values and is commonly used in lift vehicles, trucks, trains, and various industries.

The voltage applied to either the field or rotor windings can regulate the speed of an independently excited motor, allowing for independent control of the armature and field voltage to manage the motor's speed.

2.2.2. Shunt Wound

A shunt wound motor is characterized by the field winding running in parallel with the armature, as illustrated in Fig. 2.3. The current sent to the motor is bifurcated into two pathways: one traverses the shunt field winding, while the other proceeds through the armature. The shunt motor offers optimal speed regulation, efficient reversing control, and minimal starting torque, making it ideal for belt-driven applications in industrial and automotive settings. It possesses the benefits of easy control performance, high availability, continuous operation, extensive control range, and low velocities [7].

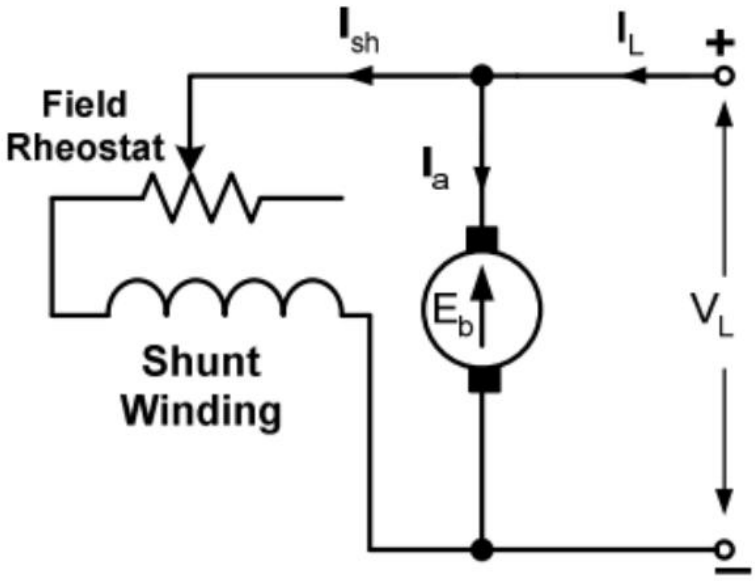

Figure 2.3: Circuit of shunt wound motor

2.2.3. Series Wound Motor

A series motor is characterized by the field winding being linked in series with the armature, enabling the whole current drawn by the motor to go through both the field winding and the armature. The connection diagram is shown in Figure 2.4. This motor offers strong starting torque, straightforward construction, ease of design, simple maintenance, cost-effectiveness, and

favorable overload torque characteristics. The drawback is that the motor reaches perilously high speeds when operating without a load. The motor's speed adjustment is somewhat challenging.

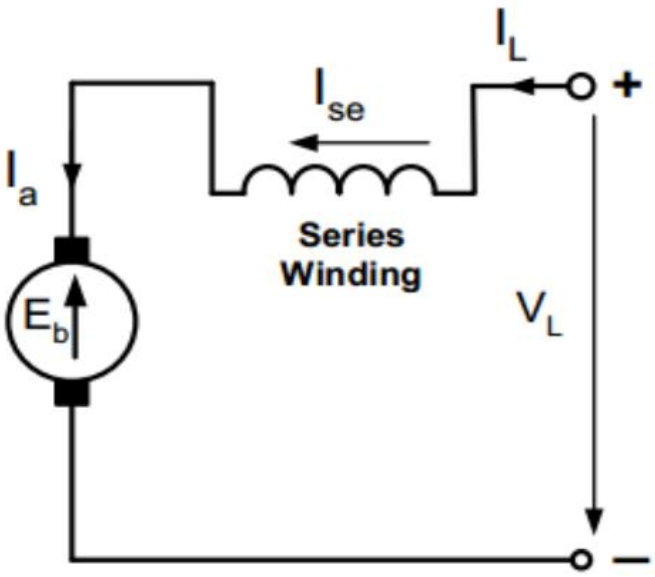

Figure 2.4: circuit of series-wound DC motor

2.2.4. Compound Wound Motor

A compound wound motor features both series and shunt windings, which can be configured as either short shunt or long shunt with the armature winding, all powered by the same source. The series field offers superior starting torque, while the shunt field enables enhanced speed regulation. The circuit of the compound-wound DC motor is illustrated in Figure 2.5.

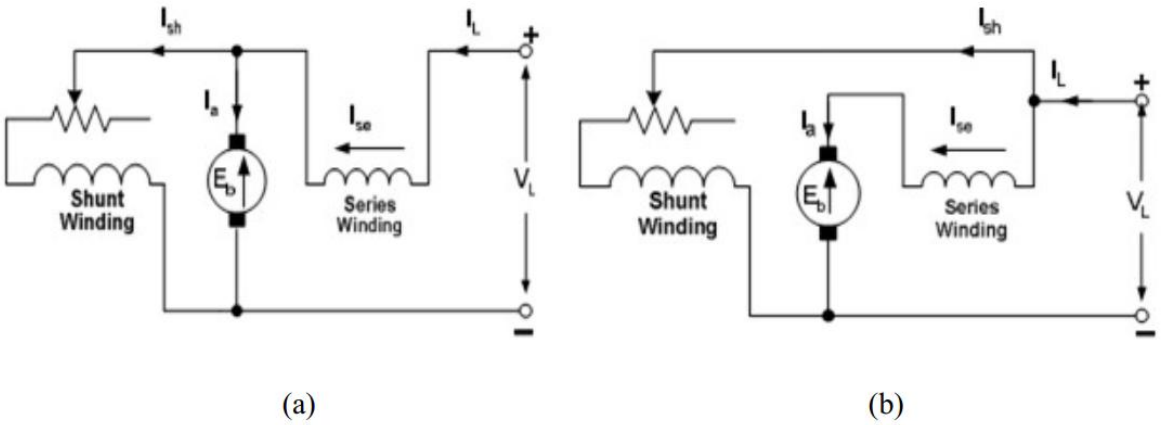

Figure 2.5: Circuit of compound wound DC motor, (a). Short shunt and (b). Long shunt

2.3 Speed Control of Separately Excited DC Motor

DC motors are often used in industrial applications, robotics, and household appliances due to their great reliability, versatility, and cost-effectiveness. The speed of a DC motor can be adjusted above or below its rated value using several approaches [18].

A separately excited DC motor consists of two components: the rotor and the stator. The stator comprises field winding, whereas the rotor, usually referred to as the armature, contains armature winding. When both the armature and field are powered by a DC supply, current traverses the windings, generating magnetic flux that is proportional to the current. The interaction between the field flux and the armature flux produces rotor rotating in the motor.

The speed of a DC motor can be controlled by regulating the field flux, the armature resistance, or the terminal voltage provided to the armature circuit. The three predominant methods for speed regulation are field resistance control, armature voltage control, and armature resistance control. In this thesis work, I used armature voltage [18].

2.3.1 Field Resistance Control Method

In the resistance control method, a series resistance is added into the shunt-field circuit of the motor in order to change the flux by regulating the field current. An increase in field resistance is theoretically anticipated to elevate the load speed of the motor and enhance the slope of the torque-speed curve [18].

2.3.2 Armature Voltage Control Method

In the armature voltage control method, the voltage supplied to the armature circuit is adjusted without altering the voltage supplied to the motor's field circuit. Consequently, the motor must be independently stimulated to implement armature voltage control. As the armature voltage is elevated, the no-load speed of the motor rises, nevertheless the direction of the torque-speed curve remains constant due to the maintenance of a constant flux [18].

2.3.3 Armature Resistance Control Method

The armature resistance control is a less frequently used approach for speed control, where an external resistance is introduced in series with the armature circuit. An elevation in armature resistance leads to a substantial augmentation in the slope of the motor's torque-speed characteristic, while the no-load speed remains unchanged [18].

2.3.4 Pulse Width Modulation (PWM)

Pulse-width modulation (PWM) is a modulation technique that adjusts the pulse width, specifically the pulse duration, according to the information from the modulator signal. This modulation technique primarily enables the regulation of power supplied to electrical equipment, particularly inertial loads like motors, however it can also encode information for transmission.

The mean value of voltage (and current) supplied to the load is regulated by rapidly toggling the switch between the supply and the load. The extended duration of the switch being activated relative to the deactivated intervals results in an increased power supply to the load. The PWM switching frequency must much exceed the rate that would impact the load, namely the device utilizing the power [18].

2.4 Mathematical Model of Separately Excited DC Motor

Several types of DC motors are widely used in industry, including brushed DC motors and brushless DC motors. This mathematical model will provide a complete analysis of a separately stimulated DC motor. The term "separately excited DC motor" indicates that the power supply is provided independently to both the field and armature windings. The primary distinguishing characteristic of these sorts of DC motors is that the armature current cannot cross the field winding, as the field winding is powered by a separate external source of DC current [19], as illustrated in the figure below.

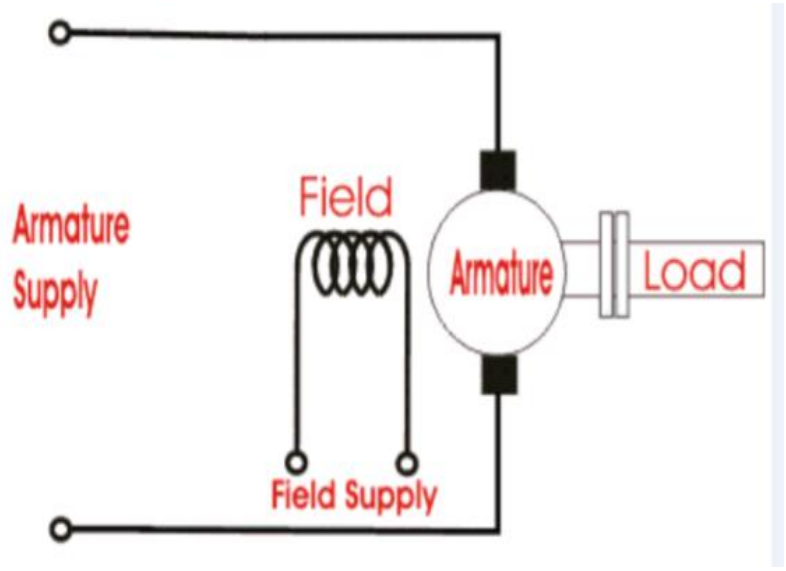

Figure 2.6: separately excited DC motor [19]

The rotor and the shaft are assumed to be rigid.

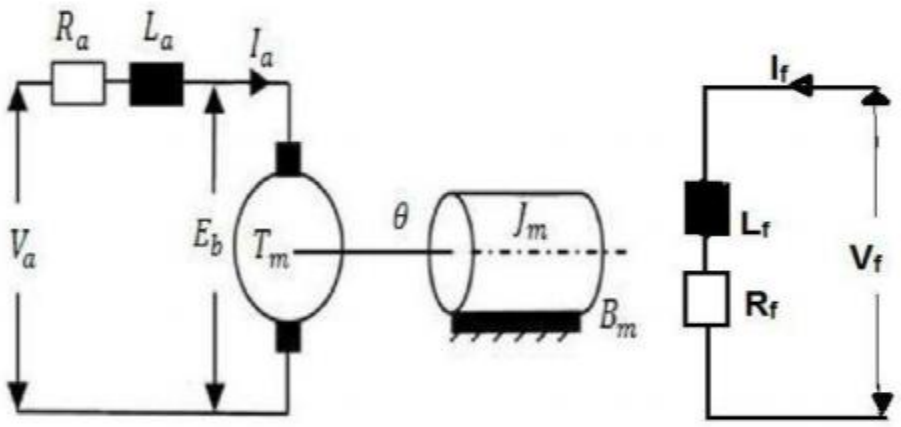

Figure 2.7: Models of DC motor [7]

As per Kirchhoff's voltage rule, the electrical equation controlling the DC motor is

$$R_a i_a(t) + L_a\, di(t)/dt + V_b(\mathrm{t}) = V_s(\mathrm{t}) \quad (1)$$

Where $i_a(\mathrm{t})$ is the armature currents, $V_b(\mathrm{t})$ is the back emf voltage and $V_a(\mathrm{t})$ is the armature voltage source. The back emf voltage $V_b(\mathrm{t})$ is directly related to the angular velocity $\omega(t)$ of the rotor in the motor,

$$V_b(\mathrm{t}) = k\phi\omega(t) = K_b\, \omega(t) \quad (2)$$

Where K_b is the back emf constant. Furthermore, the motor generates a torque T_M proportional to the armature current, given as

$$T_M(t) = k\phi\, i_a(t) = K_t\, i_a(\mathrm{t}) \quad (3)$$

In addition, if the DC motor is used to drive an external torque $T_L(t)$ of payload, then its mechanical behavior is described as

$$\mathrm{J_M}\, \mathrm{dw(t)/dw\,(t)} + B_M\, \mathrm{w(t)} = T_M(t) - T_L(t) \quad (4)$$

Where $\mathrm{J_M}$ is the rotor moment of inertia and B_M is the frictional coefficient.

Based on (1), (2). (3) And (4), the dynamic equation of the DC motor can be expressed as

$$R_a i_a(t) + L_a\, di(t)/dt + K_b\, \omega(t) = V_s(\mathrm{t}) \quad (5)$$

$$J_M\, \mathrm{dw(t)/d\,t} + B_M\ \mathrm{w(t)} - K_t\, i_a(\mathrm{t}) = -T_L(t) \quad (6)$$

Taking Laplace transform of the motor's armature voltage equation

In order to create the block diagram of system initial conditions are zero and Laplace transform is implemented to the equations. i.e.

$$V_s(s) = R_a I_a(s) + SL_a . I_a(s) + V_b(s) \quad (7)$$

$$T_M(s) = SJ_M w(s) + B_M w(s) + T_L(s) \quad (8)$$

$$I_a(s) = \frac{(Va - Vb)}{(R_a + L_a S)} \quad (9)$$

Taking Laplace transform of the motor's mechanical equation

$$T_M = J_M S w(s) + B_M w(s) + T_L \quad (10)$$

$$w(s) = \frac{T_M - T_L}{J_M s + B_M} \quad (11)$$

The relation between rotor shaft, speed and applied armature voltage is represented by transfer function.

Upon simplification of the above motor model, the resultant transfer function will be

$$W(s)/V_s(s) = \frac{K_t}{s^2 J_M L_a + s(B_M L_a + J_M R_a) + R_a B_M + K_t K_b} \quad (12)$$

The correlation between position and speed is

$$X(s) = \frac{1}{s} w(S) \quad (13)$$

This equation for the DC motor is shown in the block diagram in Figure 2.8

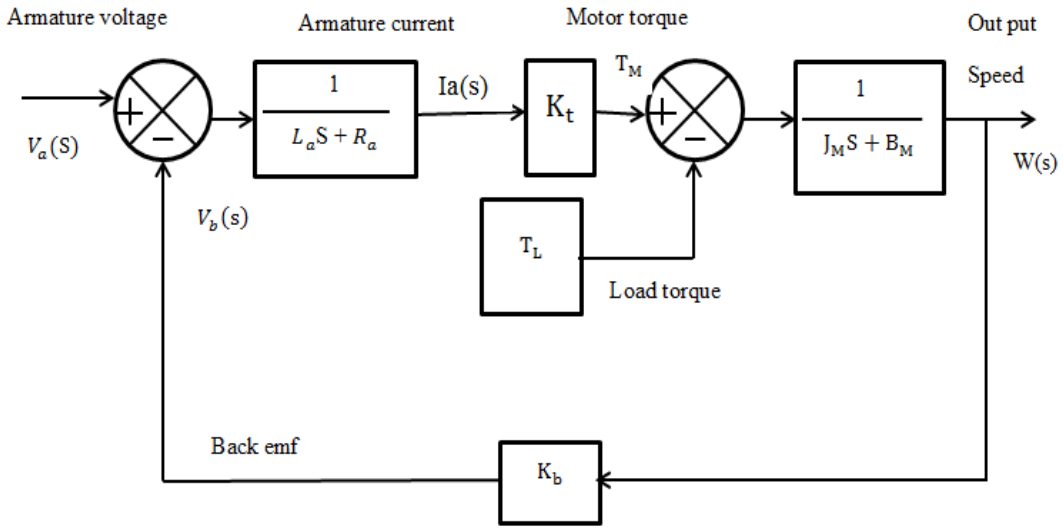

Figure 2.8: block diagram of DC motor

The rotor and the shaft are assumed to be rigid. The following values for the physical parameters of DC motor have been used in this thesis work [29]:

Table 2.1 Specifications of the DC Motor Parameters [29].

Description of the parameter	Parameter value
Armature resistance (R_a)	0.5Ω
Armature inductance (L_a)	0.02 H
Armature voltage (V_a)	200 V
Mechanical inertia (J_M)	0.1 Kg.m^2
Friction coefficient (B_M)	0.008 NM/rad/sec
Back emf constant (K_b)	1.25 V/rad/sec
Motor torque constant(K_t)	1 NM/A
Rated speed	1500 rpm
Rated power	12hp

CHAPTER THREE

Controller Design and Analysis

This chapter presents The development of speed control for a separately excited DC motor is, first, The design of Buck Regulator and conventional controller (PID) for training data generation is followed by the design of a fuzzy logic controller and an intelligent Adaptive Neuro-Fuzzy Inference System (ANFIS) controller.

3.1. Buck Regulator

A DC-DC converter, often known as a chopper, is a power electronic device that transforms a fixed DC supply into a variable voltage DC source. In industrial applications, it is frequently necessary to transform a fixed DC voltage level into numerous voltage levels. A DC converter might be seen as the DC equivalent of a transformer, as a transformer alters AC voltage levels, while a DC-DC converter performs a similar function within the DC domain. DC converters have numerous industrial applications. They are widely used for the regulation of traction motors. They offer fast acceleration and rapid dynamic responsiveness. DC converters are currently employed globally in fast transit systems. These are also used for trolley cars, maritime hoists, forklift trucks, and mine transporters. Future electric vehicles are expected to utilize choppers for speed regulation and braking. As the name suggests the output voltage of buck regulator is less than the input voltage [30] .

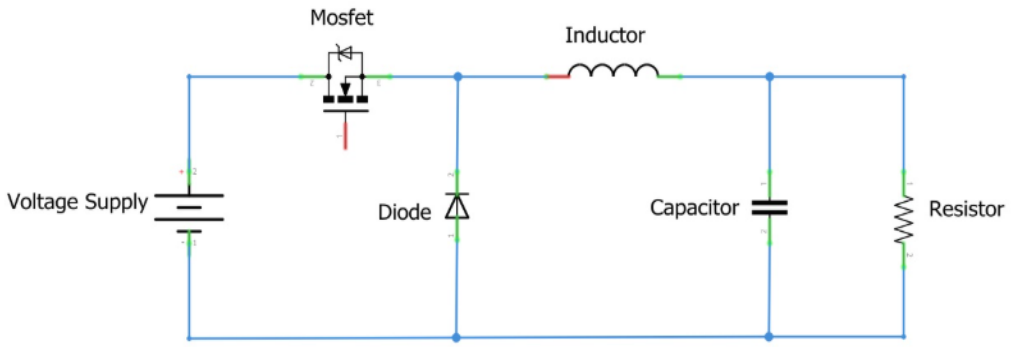

Figure 3.1: Buck converter [30]

3.1.1 Designing the Buck Converter

Mathematical relationship between input and output voltage is given by

$$V_0 = D\ V_{in} \tag{3.1}$$

Where "D" is termed as duty cycle of switching signal. Its value varies from 0 to 1.

Determine the Output Voltage (V_0) and Current (I_{out}) V_0 is given as the Armature voltage,

$V_0 = 200\text{V}$ To find Current (I_{out}), we can use the rated power and voltage.

Rated power(P_{rated}) = 12hp = 12hp × 745.7 w/hp= 8948.4W. (3.2)

Assuming the motor operates at its rated power with the armature voltage,

$$(I_{out}) = \frac{P_{rated}}{V_a} = \frac{8948.4\text{W}}{200\text{V}} = 44.74\text{ A} \tag{3.3}$$

the buck converter needs to supply approximately 200V and up to 44.74 A.

to find Load resistance (R_0) using Output Voltage and output Current.

$$(R_0) = \frac{\text{V}_0}{\text{I}_{\text{out}}} = \frac{200\text{ V}}{44.74\text{ A}} = 4.47\Omega \tag{3.4}$$

I Chose an Input Voltage (V_{in}), for a buck converter, V_{in} must be greater than V_0 , Let's assume V_{in} = 400V for a good voltage difference.

Determine the Duty Cycle (D): For a buck converter in continuous conduction mode (CCM):

$$D = \frac{V_0}{V_{in}} = \frac{200}{400} = 0.5 \tag{3.5}$$

Select Switching Frequency (f_s): a higher switching frequency allows for smaller inductor and capacitor sizes but increases switching losses. I chose a typical frequency, f_s =20kHz.

Calculate Inductor (L)

the inductor is critical for filtering the current. We need to choose an appropriate ripple current (ΔI_L). A common choice is to allow 20% to 40% of the maximum output current as ripple. I chose for 30% ripple.

$$\Delta I_L = 0.30 \times I_{out} = 0.30 \times 44.742\text{ A} = 13.42\text{ A} \tag{3.6}$$

The formula for the inductor in a buck converter is:

$$\text{L} = \frac{V_0 \times (1-\text{D})}{f_s \times \Delta I_L} \tag{3.7}$$

$$\text{L} = \frac{200\ v\ \times (1-0.5)}{20{*}10^3\ Hz \times 13.42\text{ A}} = \frac{200\times 0.5}{20000 \times 13.42} = \frac{100}{268400} = 0.0003726 = 372.6\ \mu H$$

Calculate Output Capacitor (C): The output capacitor filters the output voltage ripple. A common choice is to limit the ripple voltage (ΔV_{out}) to 1% to 5% of the output voltage. I chose for 1% ripple.

$$\Delta V_{out} = 0.01 \times V_{out} = 0.01 \times 200\ \text{V} = 2\text{V} \tag{3.8}$$

The formula for the output capacitor in a buck converter is:

$$C = \frac{\Delta I_L}{8 \times f_s \times \Delta V_{out}} \tag{3.9}$$

$$C = \frac{13.42}{8 \times 20 \times 10^3\ Hz \times 2\ \text{V}} = \frac{13.42}{320000} = 0.0000419\ \text{F} = 41.9\ \mu\text{F}$$

The buck converter can be modeled using state-space averaging and in continuous conduction mode (CCM). The output voltage-to-duty cycle transfer function $G_{vd}(s)$ is given by:

$$G_{vd}(s) = \frac{V(S)}{D(S)} \tag{3.10}$$

During T_{ON} (switch closed):

Voltage across the inductor $V_L = V_s - V_O$

$$di(t)/dt = \frac{(V_s - V_O)}{(L)} \tag{3.11}$$

During T_{OFF} (switch open):

$$di(t)/dt = \frac{-V_O}{L} \tag{3.12}$$

For steady-state operation, the net change in inductor current over one cycle is zero:

$$(Vs - Vo) * T_{ON} = Vo * T_{OFF} \tag{3.13}$$

$$Vs * T_{ON} = Vo\ (T_{ON} + T_{OFF}) = Vo\ (T)$$

$$D = \frac{T_{ON}}{T} \tag{3.14}$$

Substitute of equation (3.14) into equation (3.13)

$$Vo = \frac{Vs\ T_{ON}}{T} = D \cdot Vs \tag{3.15}$$

to find The output voltage-to-duty cycle transfer function

The output voltage-to-duty cycle transfer function is given by:

$$G_{vd}(s) = \frac{V(S)}{D(S)} \tag{3.16}$$

State variables: Let I_L = inductor current and V_C are state variable:

Switch ON (duty D):

$$\frac{\mathrm{d}\,\mathrm{I_L}}{\mathrm{dt}} = \frac{V_{in} - V_c}{\mathrm{L}} \tag{3.17}$$

$$\frac{\mathrm{d}\,V_c}{\mathrm{dt}} = \frac{\mathrm{I_L} - V_{c\,/R}}{\mathrm{C}} \tag{3.18}$$

Switch OFF (1−D):

$$\frac{\mathrm{d}\,\mathrm{I_L}}{\mathrm{dt}} = \frac{-V_c}{\mathrm{L}} \tag{3.19}$$

$$\frac{\mathrm{d}\,V_c}{\mathrm{dt}} = \frac{\mathrm{I_L} - V_{c\,/R}}{\mathrm{C}} \tag{3.20}$$

Averaging over one switching period and Linearize about the steady operating point $\mathrm{I_L}$=I, V_c=V, the small-signal averaged linearized state equations

$$\frac{\mathrm{d}\,\mathrm{I(t)}}{\mathrm{dt}} = \frac{V_{in} d(t)}{\mathrm{L}} - \frac{\mathrm{v}(t)}{\mathrm{L}} \tag{3.21}$$

$$\frac{\mathrm{d}\,\mathrm{V(t)}}{\mathrm{dt}} = \frac{\mathrm{I(t)}}{\mathrm{C}} - \frac{\mathrm{v}(t)}{\mathrm{RC}} \tag{3.22}$$

Take the Laplace transform (zero initial conditions)

$$\mathrm{SI(S)} = \frac{V_{in} D(S)}{\mathrm{L}} - \frac{\mathrm{V}(S)}{\mathrm{L}} \tag{3.23}$$

$$\mathrm{SV(S)} = \frac{\mathrm{I(S)}}{\mathrm{C}} - \frac{\mathrm{V}(S)}{\mathrm{RC}} \tag{3.24}$$

Substitute equation (3.23)into Equation (3.24)

$$V_{in}\,\mathrm{D(S)} = \mathrm{V(S)}\left(1 + \frac{\mathrm{L}}{\mathrm{C}}\,\mathrm{S} + \mathrm{LC}\,\mathrm{S}^2\right)$$

(3.24)

Then

$$\mathrm{G_{vd}(s)} = \frac{\mathrm{V(S)}}{D(S)} = \frac{V_{in}}{\mathrm{s2\ LC} + \mathrm{s}\frac{L}{\mathrm{R}} + 1} \tag{3.25}$$

$$\mathrm{G_{vd}(s)} = \frac{400}{\mathrm{s2}\ (1.56*10-8) + \mathrm{s}(5.76*10-5) + 1}$$

MOSFET/IGBT: The switch needs to withstand $V_{in}$when off and carry, I_{out} when on.

Voltage rating: > V_{in}, so 400V,A 600V or 800V rated device would be suitable. I chose Voltage rating 400 V

$$\text{Current rating} = I_{out(\max)} + \frac{\Delta I_L}{2} \tag{3.26}$$

$$\text{Current rating} = 44.742 + \frac{13.42}{2} = 51.45\ \text{A.}$$

Diode (Freewheeling Diode):

Voltage rating: > V_{in}, so > 400V. Current rating = 51.45 A

$$\text{Average current} = I_{out(\max)} \times (1-D) \quad (3.27)$$

$$\text{Average current} = 44.742 \times (1-0.5) = 22.37 \text{ A}$$

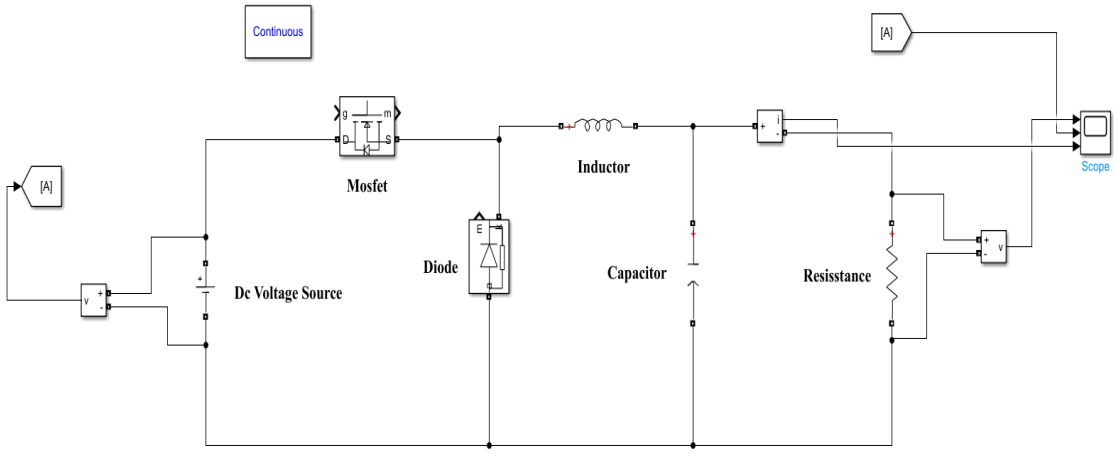

Figure 3.2: Structure of Buck Converter

3.2. PID Controller

The PID (Proportional-Integral-Derivative) controller is the most prevalent controller in industrial and other applications due to its simplicity, durability, and effective practical implementation. The controller's versatility enables its application in many different situations. The configuration of the PID controller is shown in Figure 3.3.

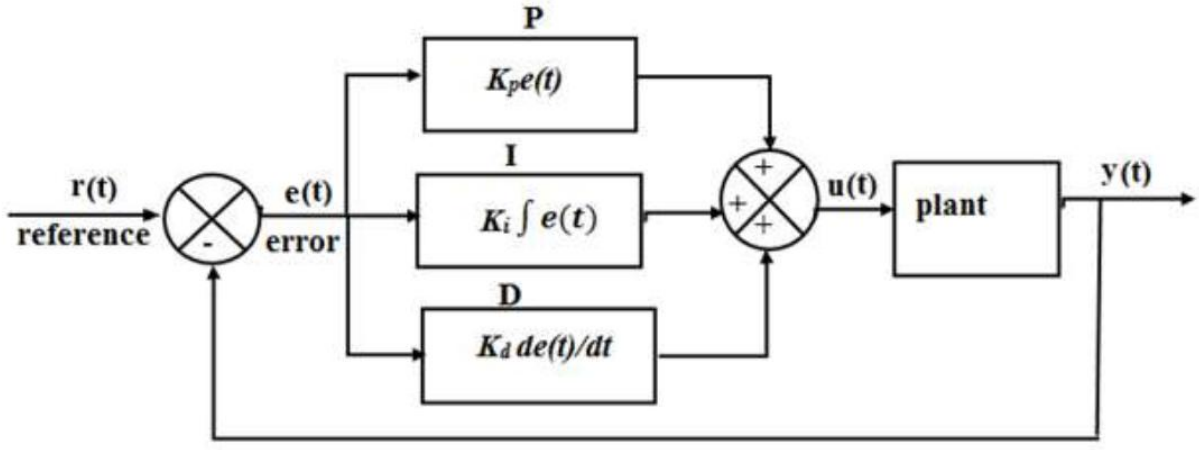

Figure 3.3: Structure of parallel PID controller [20]

The PID controller integrates three fundamental control mechanisms into a single integrated system. The primary role of the controller is to produce a control signal u that ensures the plant

output correlates with the reference or command signal. The parallel configuration of a PID controller represented in Figure 3.3 has the following transfer function

$$C(s) = K_P + \frac{K_d}{S} + \mathrm{K_d\,s} = K_P\left(1 + \frac{\mathrm{Kd}}{Tis} + \mathrm{T_d\,s}\right) \quad (3.28)$$

where, *Kp*= Proportional Gain, Ki = Integral Gain, *Kd* =Derivative gain

$\mathrm{T_i}$ = Reset Time =K_P/K_i and Td = Rate time or derivative time= $\mathrm{K_d}/K_P$

If K_i and $\mathrm{K_d}$ are zero, we have a simple P controller, if only $\mathrm{K_d}$ is zero, we have a PI controller and if only K_i is zero, we have a PD controller.

The control signal U(s) is therefore given by,

$$\mathrm{U(S)} = \left(K_P + \frac{K_i}{S} + K_d\mathrm{s}\right) E(S) \quad (3.29)$$

Let e be the error signal defined by e = r - y, where r represents the reference signal and y signifies the output of the plant. $K_d\mathrm{S}$ represents the transfer function of the derivative controller; however, it is an incorrect transfer function, making practical implementation challenging. Consequently, in practice, the derivative term is adjusted as:

$$D = \frac{K_d}{1+\frac{K_d S}{N}} \quad (3.30)$$

N, which varies from 3 to 10, is specified by the manufacturer and is referred to as the taming factor. This taming factor facilitates the construction of the controller and restricts the amplification of high-frequency noise [21]. Therefore, the control signal is given by:

$$\mathrm{U(S)} = \left(K_P + \frac{K_i}{S} + \frac{K_d}{1+\frac{K_d S}{N}}\right) E(S) \quad (3.31)$$

The control signal, U(s), provided to the plant is the weighted sum of the products of the gains K_P, K_d , and K_i with the error signal, the rate of change of the error, and the integral of the error signal, respectively. Each PID gain influences the plant's reaction distinctly. The effects of the gains are summarized in Table-3.1.

Table-3.1: Effects of PID gains [21]

	Effect on the performance measures			
PID gains	Overshoot	Settling time	Steady state error	Rise time
Increasing K_P	Increase	Increase	Decrease	Faster
Increasing K_i	Increase	Increase	Eliminate	Slower
Increasing K_d	Decrease	Decrease	No effect	Minor

Despite the significance of the PID controller in industrial and other applications, control engineers face issues in tuning the necessary gains to provide stability, optimal transient response, and steady-state performance of the system. Numerous prescriptive techniques and guidelines are employed in PID gain adjustment. The predominant PID tuning technique is that introduced by Ziegler and Nichols in the 1940s [22].

3.2.1 Ziegler-Nichols First PID tuning method

The first Ziegler-Nichols tuning method, also known as the closed-loop or ultimate cycle method, This is a more systematic, empirical method for tuning. It's often used for systems that can be brought to the point of marginal stability (continuous oscillation).This method is based on the principle of pushing the system to its limit of stability to determine its fundamental oscillatory characteristics. The following steps are used to find optimal values for K_P, K_i and K_d [22].

Set the Controller to P-Only Mode: Start by disabling the integral (K_i) and derivative (K_d) actions. This is done by setting K_i to zero and K_d to zero.it left with a simple proportional controller.

Increase Proportional Gain (K_P) until Sustained Oscillations: With the system running in a closed loop, gradually increase the proportional gain (K_P) from a low value. The system will initially become more responsive. Continue increasing K_P until the process variable begins to oscillate continuously with a constant amplitude. The system is now at its marginal stability limit.

Record Key Values: Once I have achieved stable, constant oscillations, I need to record two key values:

Ultimate Gain (K_u): This is the value of K_P at which the sustained oscillations occur.

Ultimate Period (T_u): This is the time it takes for one full cycle of oscillation.

Use the Tuning Table: With Ku and Tu, I can use the Ziegler-Nichols tuning table to calculate the initial values for a P, PI, or PID controller. The table provides a quarter-wave decay ratio, which means each successive peak in the response is a quarter of the size of the previous one. This is a good starting point for many industrial processes.

Table-3.2: Ziegler and Nichols method controller gains

Type of controller	Proportional Gain (K_P)	Integral Gain (K_i)	Derivative Gain (K_d)
P	0.5 K_u	0	0
PI	0.45 K_u	$\frac{1.2\ K_p}{T_u}$	0
PID	0.6 K_u	$\frac{1.2\ K_p}{T_u}$	$\frac{T_u * K_p}{8}$

Multiple gain values have been evaluated to determine the optimal values for K_P, K_i and K_d. The optimal gain value combinations occurs when the system operates with minimal overshoot, minimal steady-state error, and minimal settling time. The comprehensive simulation circuit for the PID controller. Using a PID controller, we examined the speed, steady-state error (ess), rising time (t_r), settling time (t_s), and overshoot of the motor under three distinct loads with an applied voltage of 200 DC volts.

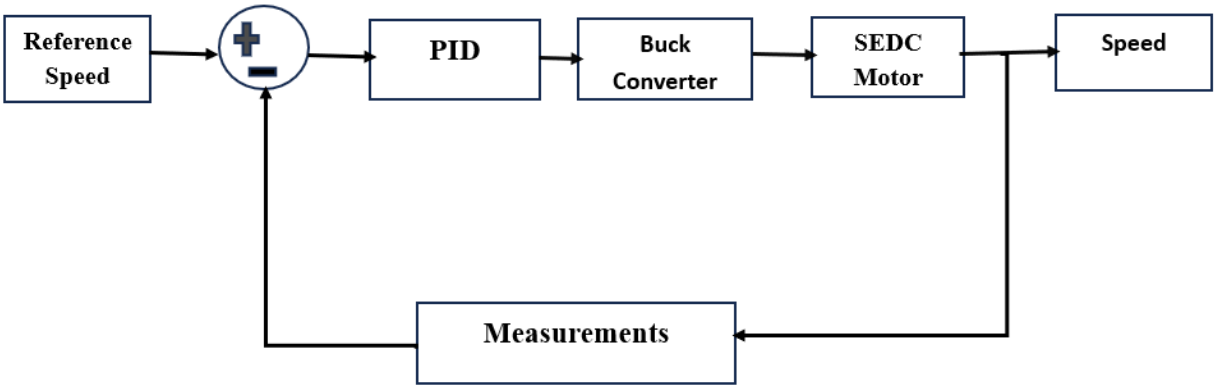

Figure 3.4: Block diagram of DC Motor with PID controller

The following values for the physical parameters such as PWM(Pulse) Generator, Buck Converter , armature resistance(R_a), armature voltage (V_a), armature inductance (L_a), Mechanical inertia

(J_M), Friction coefficient (B_M), Back emf constant (K_b), Motor torque constant (K_t) of DC motor have been used in this thesis work [29].

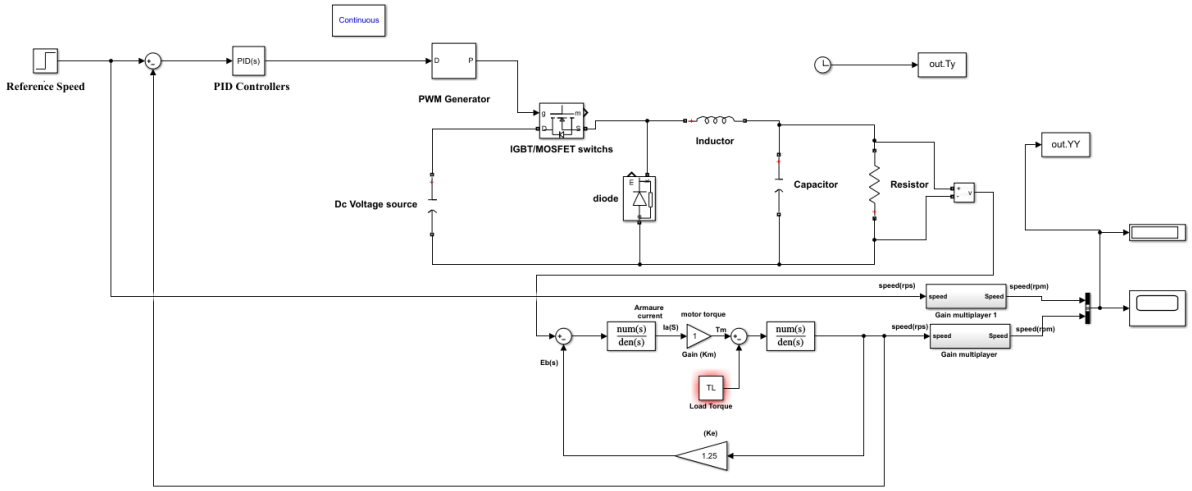

Figure 3.5: PID controller modeling system

3.3. Fuzzy Inference System (FIS)

The concept of a fuzzy inference system parallels the human cognitive process of perception and reasoning; in contrast to conventional control strategies, which operate on a point-to-point basis, a fuzzy inference system functions on a range-to-point or range-to-range basis. The result of a Fuzzy inference system is obtained by the fuzzification of both inputs and outputs utilizing the corresponding membership functions. An accurate input will be transformed into the various components of the corresponding membership functions according to its value. From this perspective, the output of a fuzzy logic controller is determined by its membership functions, which can be regarded as a range of inputs. [24]. A simple block diagram of a fuzzy logic system is shown in in Figure 3.6.

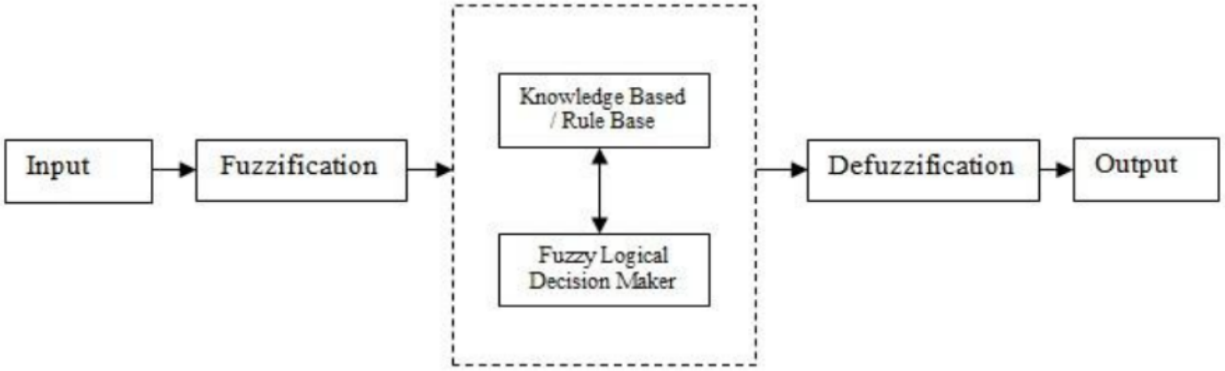

Figure 3.6: Structure of Fuzzy Logic Controller [24]

3.3.1 Input Variable

An input variable to the Fuzzy Inference System (FIS) is an error and its derivative. This variable must be maintained at a specific value known as the set point or reference signal to ensure system stability and prevent oscillation. Augmenting the quantity of input variables enhances the complexity and dependability of the system [25].

3.3.2 Fuzzification

This method transforms the precise input into fuzzy linguistic values. The initial stage in constructing a fuzzy controller is to determine which state variables that characterize the system's dynamic performance will serve as the input signals to the controller. Fuzzy logic typically employs language variables rather than precise or numerical variables. The conversion of a numerical variable (crisp variable) into a linguistic variable (fuzzy variable) is termed Fuzzification. The inputs commonly utilized for fuzzy controllers include state error, integral of state error, and derivative of state error, among others [25].

3.3.3 Rule Base and Inference Engine

A collection of rules is referred to as a rule base. The rules are structured in a "If Then" manner, with the "If" component referred to as the conditions and the "Then" component as the conclusion. The computer can implement the rules and calculate a control signal based on the measured input error (e) and the change in error (Ce). The fuzzy engine serves as the core of a fuzzy logic controller, enabling the simulation of human decision-making through fuzzy ideas and the derivation of fuzzy control actions via fuzzy implication and the principles of inference in fuzzy logic. The fuzzy inference engine facilitates rule inference, allowing for the seamless integration of human experience via linguistic rules [25].

- **Fuzzy inference model**

  (A), Mamdani model; Mamdani-type inference, as specified for the toolbox, predicts that the output membership function comprises fuzzy sets. Following the aggregation procedure, a fuzzy set for each output variable requires defuzzification [26].

  (B), **sugeno model;** sugeno or takagi-kang, method of fuzzy inference is mostly similar with mamdami model but the different is segeno output member ship functions are either linear or constant, the rule base of segeno is like if x is A and y is B then z is F(x, y), mostly use this model if there is no expert knowledge about the system [26].

For this thesis work I have selected mamdami FL model due to suited to human input, it asks expert knowledge about the system and wide spread acceptance, simplicity case of implementation, and rules set up is if--- then---.

- **Type of membership function**

  Membership functions exhibit various shapes. These include triangular, trapezoidal, piecewise linear, Gaussian, and bell-shaped forms, among others. Altering the configuration of the membership function enables the user to optimize the system's response. The choice of the specific kind is contingent upon the particular applications. For systems requiring substantial dynamic fluctuation within a brief timeframe, a triangle or trapezoidal waveform should be employed. For systems requiring high control accuracy, the most commonly utilized membership functions in real-time implementations are triangular and trapezoidal, due to their ease of representation of the designer's concepts and minimal computational time requirements. I have used a triangle membership function [26].

3.3.4 Defuzzification

Defuzzification is used to transform the results derived from the inference mechanism into the real inputs for the plant. Defuzzification is the procedure of converting a collection of inferred fuzzy control signals through a fuzzy output window into a precise control signal. Various defuzzification strategies exist, although the center of area (COA) method is the best recognized technique which in linguistic terms can be expressed as

$$\text{Crisp Control Signal} = \frac{\text{Sum Of First Momemnts Of Area}}{\text{Sum Of Areas}} \tag{3.32}$$

For continuous system the above equation becomes

$$\mathrm{U(t)} = \frac{\int_{\cdot} U_{\mu}\,(\mathrm{u})\,du}{\int_{\cdot} \mu\,(\mathrm{u})\,\mathrm{du}} \tag{3.33}$$

For a discrete system the above equation becomes

$$\mathrm{U(t)} = \frac{\sum_{i=1}^{n} Ui_{\mu}\,(\mathrm{ui})}{\sum_{i=1}^{n} \mu\,(\mathrm{u})} \tag{3.34}$$

Where Uiis the center of relevant output membership function i and μ(ui) is area of relevant output membership function i.

In this thesis work I have selected center of area for defuzzification method because the widest used technique is the Centre of Area (COA) method and Centre of Area (COA) of defuzzification method effectively calculates the best compromise between multiple output linguistic terms.

For each type of FLC controller design, performance of the controller has been analyzed and evaluate in term of percentage of maximum overshoot (OS %), rising time, peak time, settling time and steady state error.

The error is typically the difference between the reference speed (setpoint) and the actual motor speed. The rated speed is 1500 rpm or 1500 rpm $* \frac{2\pi * rad}{60\ Sec}$ = 157.08 rad/sec

Maximum Possible Speed(no load) of SEDC is the back EMF($V_b = K_b\ \omega$) is equal to equals the armature voltage (V_a).

$$W_{max} = \frac{\mathrm{V_a}}{\mathrm{K_b}} = \frac{200\ V}{1.25\ \mathrm{V/rad/sec}} = 160 \text{ rad/sec} \tag{3.35}$$

The error can range from the negative of the maximum speed to the positive of the maximum speed. So for range of error [−160 rad/sec,160 rad/sec].

Change of error Usually, the difference between the error at the previous sampling instant and the current error. The maximum current ($\mathrm{i_a}$) can be limited by the armature resistance when the back EMF is zero (during start-up):

$$\mathrm{i_a}\ max = \frac{\mathrm{V_a}}{\mathrm{R_a}} = \frac{200\ V}{0.5\Omega} = 400 \text{ A} \tag{3.36}$$

T_{Max}=$K_t\ i_a$max = 1 NM/A* 400 A= 400 Nm

Maximum Acceleration occur under conditions of maximum applied voltage and minimal opposing torque.

$$\alpha_{\max} = \frac{T_{Max}}{\mathrm{J_M}} = \frac{400\ V}{0.1\ \mathrm{Kg.m2}} = 4000 \text{ rad/sec}^2 \tag{3.37}$$

then the maximum change in speed could be

$$\Delta W_{max} = \alpha_{\max} * \Delta t \tag{3.38}$$

ΔW_{max} =4000 rad/sec^2 * 0.01Sec = 40 rad/sec, By considering a small time step = 0.01 Sec

Range for Change of Error (Δe): [−40 rad/sec, 40 rad/sec]

Control Output (u)

Duty Cycle (D) of Buck Converter

Range for Control Output (u): [0, 1].

I used five linguistic variables for my thesis because to their intuitive rule-making capabilities, effectiveness, and robustness, which balance system performance with design and computational simplicity.

Fuzzy Input:

i) Error of speed (5 membership)

ii) Change of speed error (5 membership)

Fuzzy Output:

i) Control output (5 memberships)

Fuzzy Inference System: Mamdani

Defuzzification Method: Centroid

Rules Base: 25 rules

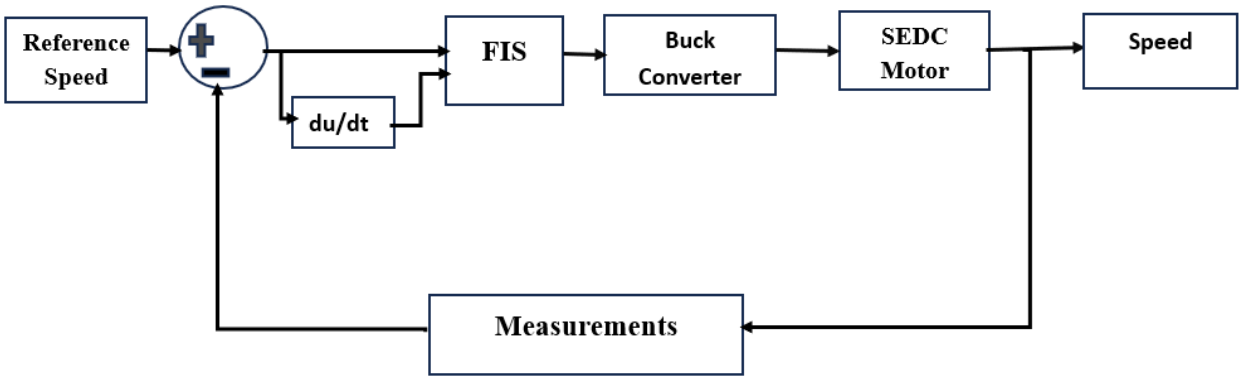

Figure 3.7: Block diagram of SEDC Motor using fuzzy logic controller

The following values for the physical parameters such as PWM (Pulse) Generator, Buck convertor, armature resistance(R_a), armature voltage (V_a), armature inductance (L_a), Mechanical inertia (J_M),

Friction coefficient (B_M), Back emf constant(K_b), Motor torque constant (K_t) of DC motor .

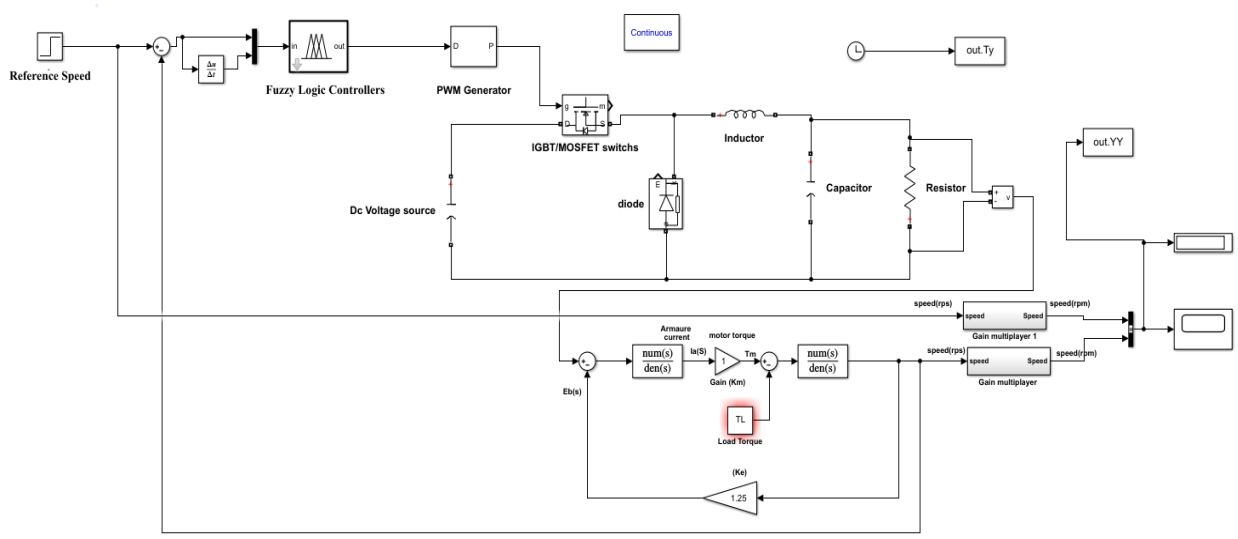

Figure 3.8: FLC controller modeling system

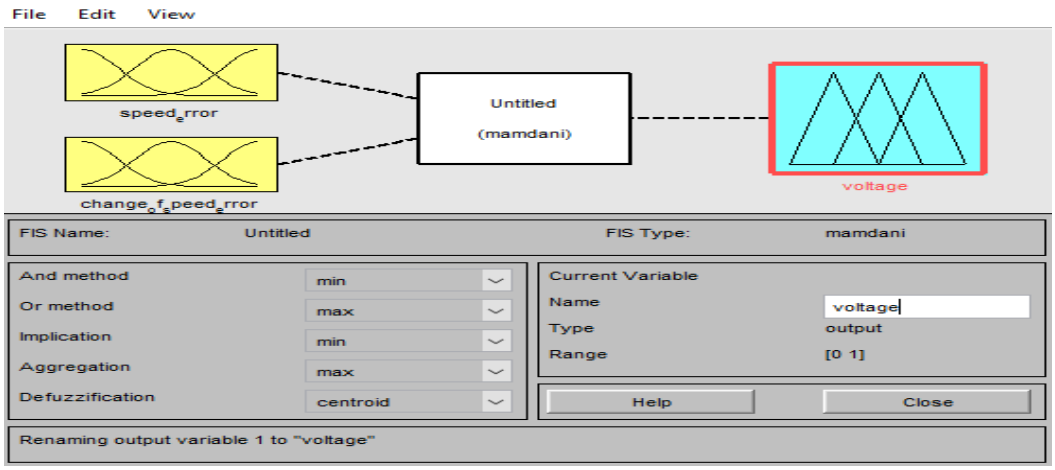

Figure 3.9: FLC controller editor

Table 3.3 shows detail of setting parameter for input error membership function. Range of error: -160 to 160.

Table-3.3: FLC controller error input membership function

Error	Value
ENL	TRIM[-160, -107, -54]
ENS	TRIM[-107, -54, -1]
EZ	TRIM[-54, -1, 52]

EPS	TRIM[-1, 52, 105]
EPL	TRIM[52, 105, 160]

Table 3.4 shows detail of setting parameter for input OF change of error membership function. Range for change of error: -40 to 40.

Table-3.4: FLC controller change of error input membership function

Change of Error	Value
CENL	TRIM[-40, -27, -14]
CENS	TRIM[-27, -14, -1]
CEZ	TRIM[-14, -1, 12]
CEPS	TRIM[-1, 12, 25]
CEPL	TRIM[12, 26, 40]

Table 3.5 shows detail of setting parameter for fuzzy output (Duty Cycle) membership function. Range of control output: 0 to 1

Table-3.5: FLC controller control output membership function

Control output	Value
VS	TRIM[0, 0.16, 0.33]
S	TRIM[0.16, 0.33, 0.5]
M	TRIM[0.33, 0.5, 0.66]
L	TRIM[0.5, 0.66, 0.83]
VL	TRIM[0.66, 0.83, 1]

Table-3.6: the Rule Base Table of the Fuzzy Controller

Δ e \ e	NL	NS	Z	PS	PL
NL	VL	VL	L	S	VS
NS	VL	L	M	VS	S
Z	L	M	S	S	M
PS	M	S	M	M	L
PL	S	VS	L	VL	VL

3.4. Adaptive Neuro- Fuzzy Inference System (ANFIS)

The Adaptive Neuro-Fuzzy Inference System (ANFIS) integrates neural networks with fuzzy logic. It gets the benefits of structured knowledge representation from fuzzy logic and the learning capacity from neural networks. Typically, in alternative FIS systems, specialized knowledge is utilized to derive the membership functions, their distributions, and to establish the fuzzy rules. ANFIS's benefit lies in its ability to autonomously derive membership functions and establish rules adaptively through the utilization of training data. ANFIS employs many neural network methods, including a hybrid learning algorithm that integrates the backpropagation technique with the least mean squares algorithm for training purposes [27].

ANFIS network control systems provide a hybrid framework for addressing complicated issues that requires intelligent systems, serving as viable alternatives to traditional model-based control methodologies. They provide effective management of prevalent difficulties related to uncertainty and unknown variations in plant characteristics and structure, hence enhancing the robustness of the control system. ANFIS exhibits a distinct mathematical framework that qualifies it as an effective universal adaptive approximator, demonstrating superior learning capabilities for comparable network complexity, resulting in significantly reduced convergence error and

enhanced nonlinear mapping. ANFIS necessitates fewer configurable parameters, and its architecture facilitates parallel processing, offers a well-organized knowledge representation, and enhances integration with alternative control design methodologies [27].

3.4.1. Architecture of ANFIS

The architecture of ANFIS is founded on a Sugeno fuzzy inference system. Within an adaptive network, one can identify two distinct categories of nodes: those that are adaptive, represented by squares, and those that are fixed, depicted as circles. In each subsequent iteration, the adaptive nodes undergo updates, whereas the fixed nodes remain unchanged. The organization and role of the neurons are contingent upon the overarching function of the network. The ANFIS architecture is capable of identifying the near-optimal membership functions of a fuzzy logic controller, facilitating the achievement of desired input-output mappings. The network utilizes a blend of the least squares method and the back propagation gradient descent method to train the parameters of the FIS membership function, aiming to replicate a specified training data set. The system reaches convergence when the training and validation errors fall within an acceptable range. The structure of ANFIS consists of five different layers [28]. These are:

- Layer1: Fuzzification layer
- Layer2: Rule layer
- Layer3: Normalization layer
- Layer4: Defuzzification layer
- Layer5: Output layer

Figure 3.4 shows two input ANFIS model structures. Input of the model are x, and y while f is the output parameter

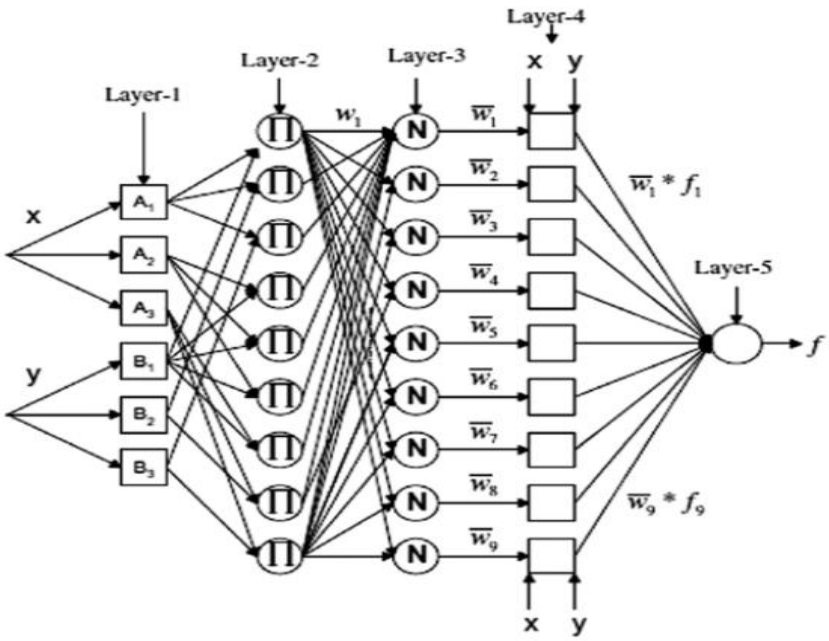

Figure 3.10: Architecture of ANFIS [28]

The fuzzification layer processes the input value and identifies the corresponding membership function associated with it. In this phase, the conventional inputs are converted into fuzzy inputs. Every node in the initial layer is a square (adaptive) node that has an estimated node function.

Rule layer: It is responsible for generating the firing strengths for the rules. Every node referred to as Π exhibits non-adaptive characteristics. The result generated by each node is derived from the multiplication of the three membership functions.

Normalization Layer: The third layer's function is to normalize the computed firing strengths by dividing each value by the total firing strength.

Defuzzification Layer:

Output layer: The sole node in this layer is a circular node that calculates the overall output as the summation of all incoming signals.

3.4.2. Back Propagation (BP)

Algorithm for learning Backpropagation is a systematic approach for training multi-layer artificial neural networks. BP employs the gradient-descent algorithm to determine network weights, aiming to minimize the error function. It can be demonstrated that BP can achieve the extremum within a finite number of epochs. The advantages of BP include that weight adjustments consistently move in the direction of decreasing the error function and that these adjustments require only localized information. Conversely, BP presents certain drawbacks. The error curve exhibits significant

complexity, characterized by numerous local minima. The algorithm's convergence is highly sensitive to the initial value. The required precision is so high that realizing weight storage is challenging [28].

3.4.3. Hybrid learning (HL) Algorithm

The hybrid learning algorithm brings together the least squares method with the back propagation technique. The operation of the network involves a forward pass followed by a backward pass. During the forward pass, outputs are computed and evaluated against the desired outputs. The discrepancy between the desired and actual output is computed. During the backward pass, this error is utilized to adjust the weights in the network to minimize the error magnitude. The forward and backward passes are iteratively performed until the error reaches an acceptable threshold [28]. The primary benefit of the hybrid algorithm is its accelerated convergence rate. This approach reduces the dimensionality of the search space in the original backpropagation method and exhibits a shorter training duration in hybrid learning [29]. In the training of ANFIS, a fuzzy system learns features from data sets and incorporates these features into the system rules. The parameters of membership functions, both premise and consequent, are adjusted during the training process to ensure that the outputs of the ANFIS model align with the actual values in the training datasets[27].

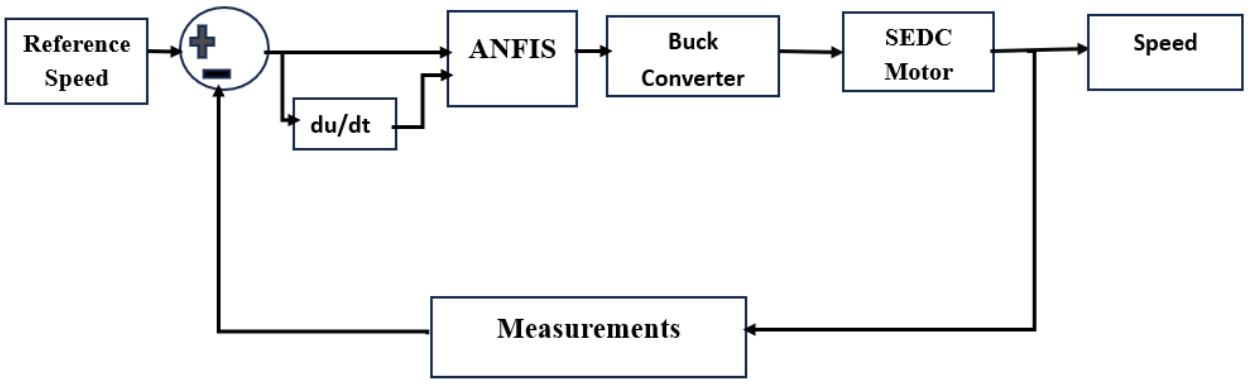

Figure 3.11: Block diagram of SEDC Motor with ANFIS

The following values for the physical parameters such as PWM (Pulse) Generator, Buck convertor, armature resistance(R_a), armature voltage (V_a), armature inductance (L_a), Mechanical inertia (J_M), Friction coefficient (B_M), Back emf constant (K_b), Motor torque constant (K_t) of DC motor have been used in this thesis work[29].

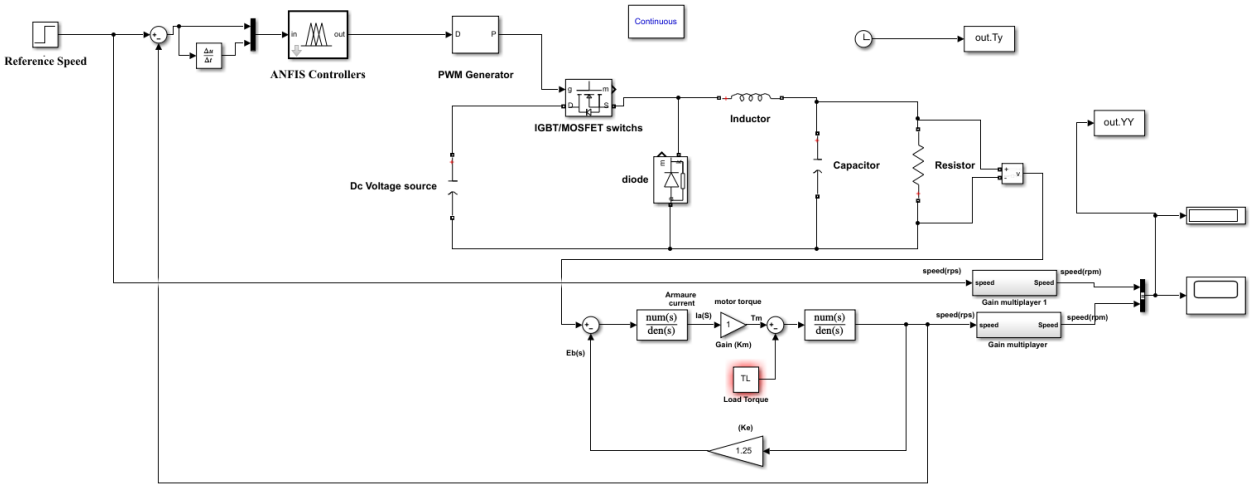

Figure 3.12: ANFIS Controller modeling system

3.4.4. Design of ANFIS in MATLAB

The implementation of Adaptive Neuro-Fuzzy Inference System (ANFIS) in MATLAB begins with data collection for training. In this study, training data is obtained from a PID controller. The objective of the training phase is to minimize the error between the ANFIS-predicted output and the actual target. This training allows the fuzzy system to learn features from the dataset and incorporate them into its rule base.

The ANFIS system is designed in MATLAB Simulink using error, change in error, and system output as inputs, with the control signal as the output. The design procedure involves the following steps:

• **Open ANFIS Editor GUI**: Launch the ANFIS interface editor.

• **Load Training Data**: Import the dataset for training.

• **Generate Membership Functions (MFs)**: The grid partitioning method is used to initialize MFs, ensuring minimal computational time and fewer rules. The hybrid optimization technique is applied for tuning.

• **Generate FIS**: Produce the Fuzzy Inference System (FIS).

The Input trained data Figure 3.13, from a conventional PID controller.

Variables - data

data

40001x3 double

	1	2	3
1	157	0	0.5217
2	157.0000	-0.0082	0.5217
3	157.0000	-0.1154	0.5217
4	157.0000	-0.4171	0.5217
5	157.0000	-1.0058	0.5216
6	156.9999	-1.9453	0.5214
7	156.9998	-3.2898	0.5213
8	156.9997	-5.0636	0.5210
9	156.9995	-7.2822	0.5207
10	156.9993	-9.9329	0.5203
11	156.9989	-12.9972	0.5198
12	156.9985	-16.4327	0.5193
13	156.9980	-20.1965	0.5188
14	156.9974	-24.2267	0.5182
15	156.9967	-28.4667	0.5176
16	156.9959	-32.8469	0.5169
17	156.9950	-37.3084	0.5163
18	156.9939	-41.7842	0.5156
19	156.9928	-46.2226	0.5150
20	156.9915	-50.5680	0.5144
21	156.9901	-54.7830	0.5138
22	156.9887	-58.8285	0.5132
23	156.9871	-62.6851	0.5127
24	156.9854	-66.3324	0.5122
25	156.9837	-69.7696	0.5117
26	156.9819	-72.9940	0.5112
27	156.9800	-76.0210	0.5108
28	156.9780	-78.8625	0.5104

Variables - data

data

	1	2	3
25	156.9837	-69.7696	0.5117
26	156.9819	-72.9940	0.5112
27	156.9800	-76.0210	0.5108
28	156.9780	-78.8625	0.5104
29	156.9760	-81.5458	0.5100
30	156.9738	-84.0923	0.5097
31	156.9717	-86.5362	0.5093
32	156.9695	-88.9028	0.5090
33	156.9672	-91.2280	0.5087
34	156.9648	-93.5359	0.5084
35	156.9624	-95.8593	0.5080
36	156.9600	-98.2173	0.5077
37	156.9575	-100.6358	0.5074
38	156.9549	-103.1263	0.5070
39	156.9523	-105.7063	0.5067
40	156.9495	-108.3784	0.5063
41	156.9468	-111.1511	0.5060
42	156.9439	-114.0186	0.5056
43	156.9410	-116.9817	0.5052
44	156.9380	-120.0275	0.5048
45	156.9349	-123.1509	0.5044
46	156.9318	-126.3344	0.5040
47	156.9285	-129.5694	0.5035
48	156.9252	-132.8365	0.5031
49	156.9218	-136.1260	0.5027
50	156.9183	-139.4189	0.5023

Variables - data

data

40001x3 double

	1	2	3
51	156.9147	-142.7071	0.5018
52	156.9111	-145.9736	0.5014
53	156.9074	-149.2135	0.5010
54	156.9035	-152.4135	0.5006
55	156.8997	-155.5726	0.5002
56	156.8957	-158.6817	0.4998
57	156.8916	-161.7361	0.4994
58	156.8875	-164.7058	0.4990
59	156.8833	-167.5851	0.4986
60	156.8791	-170.3545	0.4983
61	156.8748	-173.0182	0.4979
62	156.8704	-175.5659	0.4976
63	156.8659	-178.0108	0.4973
64	156.8614	-180.3506	0.4970
65	156.8568	-182.6052	0.4967
66	156.8522	-184.7782	0.4964
67	156.8476	-186.8934	0.4962
68	156.8428	-188.9571	0.4959
69	156.8381	-190.9948	0.4957
70	156.8332	-193.0127	0.4954
71	156.8284	-195.0350	0.4952
72	156.8234	-197.0659	0.4949
73	156.8184	-199.1264	0.4946
74	156.8134	-201.2168	0.4944
75	156.8083	-203.3539	0.4941
76	156.8032	-205.5335	0.4939
77	156.7980	-207.7678	0.4936
78	156.7927	-210.0479	0.4933

Figure 3.13: Input trained data

Figure 3.14 shows the loading and training of data to ANFIS structure. The ANFIS structure is trained with hybrid learning up to 50 epochs, with error tolerance of zero. After training the following information are obtained.

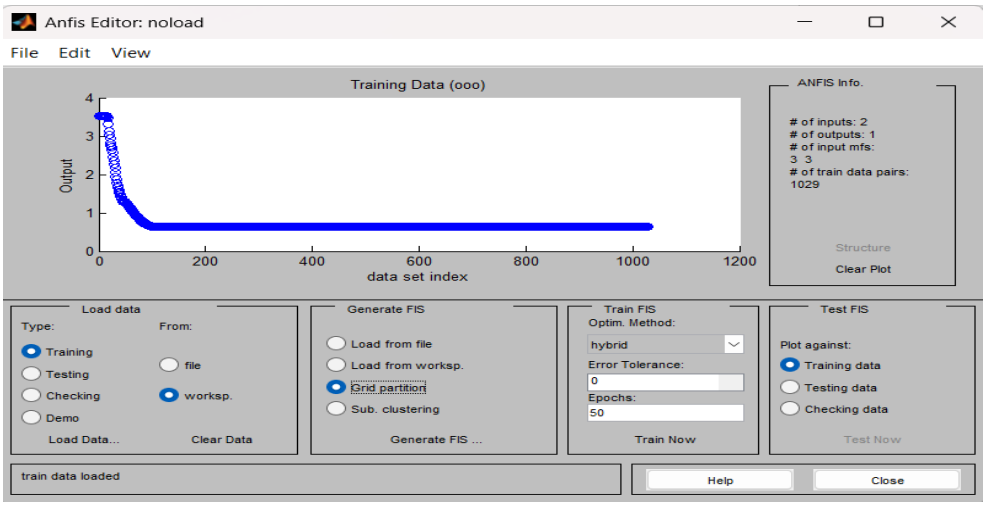

Figure 3.14: Training of data with hybrid learning method

ANFIS info:

Number of nodes: 131

Number of linear parameters: 49

Number of nonlinear parameters: 42

Total number of parameters: 91

Number of training data pairs: 1029

Number of checking data pairs: 0

Number of fuzzy rules: 49

Start training ANFIS ...

1 0.000826649

2 0.000826844

Designated epoch number reached. ANFIS training completed at epoch 2. Minimal training RMSE = 0.000826844

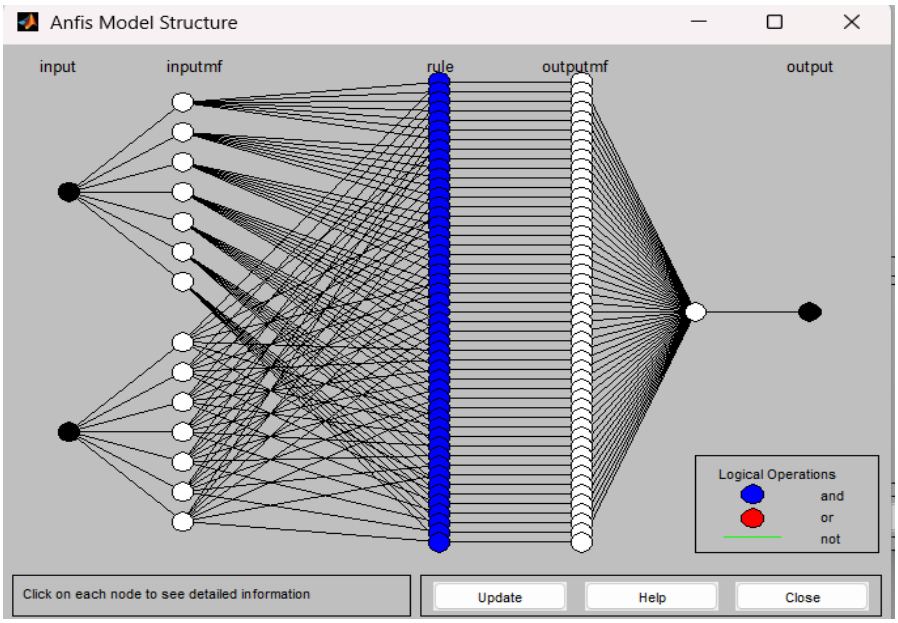

Figure 3.14: Result of the ANFIS Structure with grid partition

CHAPTER FOUR

RESULT AND DISCUSSION

This chapter discusses about the simulation results of the speed control of SEDC motor. The results and findings of the study are based on the stipulated methodology involved in the conduct of the study that highlighted the design, development, and evaluation of the development of speed control of separately excited DC motor.

4.1 Simulation of SEDCM Speed Control Without Controller

Power rated(P rated) = T full load * Rated speed (W rated) Where Prated is in watts, W rated is radian/second.

Power rated(P_{rated}) = 12 hp (12*745.7) = 8948.4 watt and W_{rated} = 1500 rpm=1500* (2π/60)= 157.079=157.1 rad/s, then we Can get T full load from rated power and rated speed.

$$\text{Torque full load} = \frac{\text{Power rated}(P_{rated})}{(\text{Rated speed (W rated)})} = \frac{8948.4}{(157.1)} = 56.97 = 57 \text{ Nm}$$

open loop modelling systems were created to model the characteristics of SEDC motors. Using applied DC voltages, by applying different load torque(full load, half load and quarter load);have measured the motor's speed.

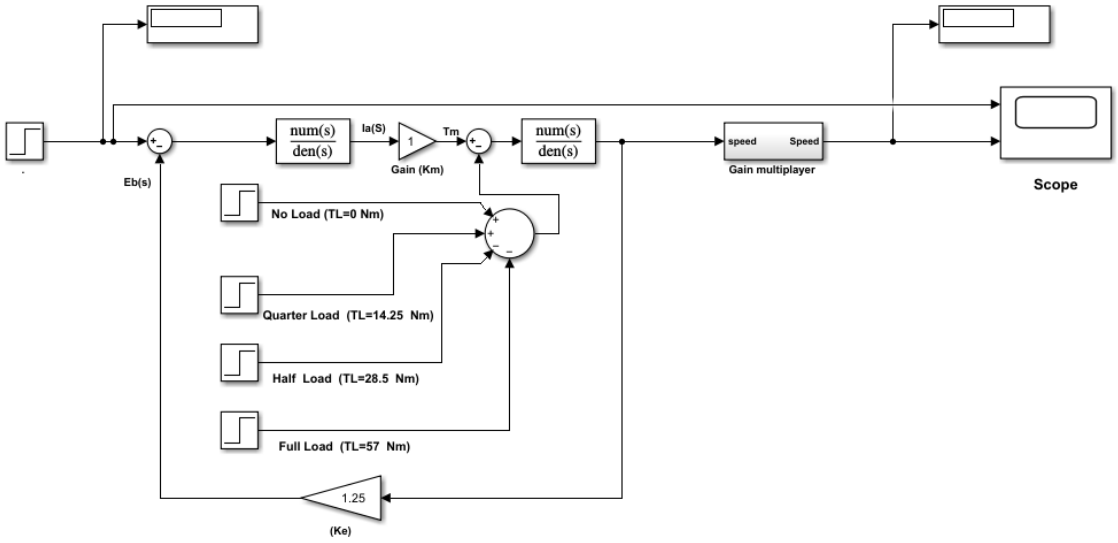

Figure 4.1: Block diagram of SEDC Motor without controller

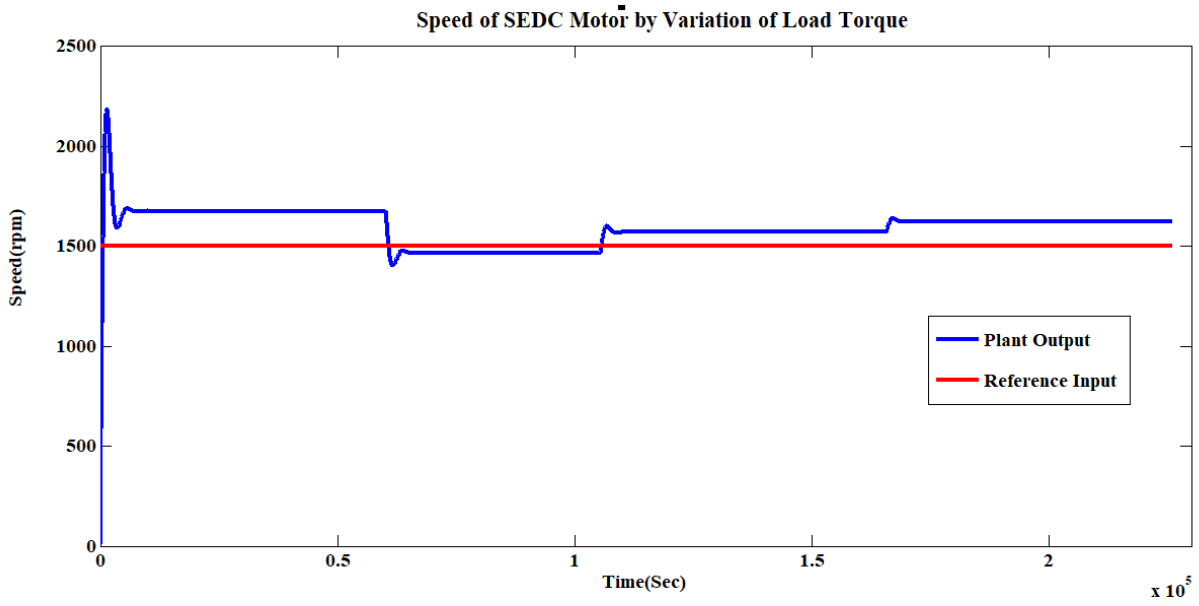

Figure 4.2: Speed of SEDC Motor by variation Load torque

Table 4.1 below shows the data for the open loop test variation load torque have been done by applying Voltage injected to the DC motor will control the speed at the SEDC motor

Table-4.1: Open loop test of input and output for SEDC motor

Load torque(TL) in NM	**Speed in RPM**
No load (TL=0 Nm)	1509 rpm
TL= 14.25 Nm (quarter load)	1455 rpm
TL= 28.5 Nm (half Load)	1401 rpm
TL= 57 Nm (full Load)	1294 rpm

Table 4.1 below shows the data for the open loop test have been done. Voltage input injected to the DC motor will control the speed at the SEDC motor.

Table-4.1: Open loop test of input and output for SEDC motor

Input voltage(V)	Speed Output (rpm)
5	37.2
10	75.44
20	150.9
30	226.3
40	301.8

50	377.7
60	452.6
70	527.9
80	603.4
90	679

By altering the armature voltage, the motor's speed may be regulated; in particular, as the armature voltage rises, the motor's speed rises, and when the armature voltage falls, the SEDC motor's speed falls.

Initially, open loop modelling systems were created to model the characteristics of SEDC motors. Using applied DC voltages, have measured the motor's speed, steady state error (ess), rise time (t_r), settling time (t_s), and overshoot at three distinct loads in this circuit.

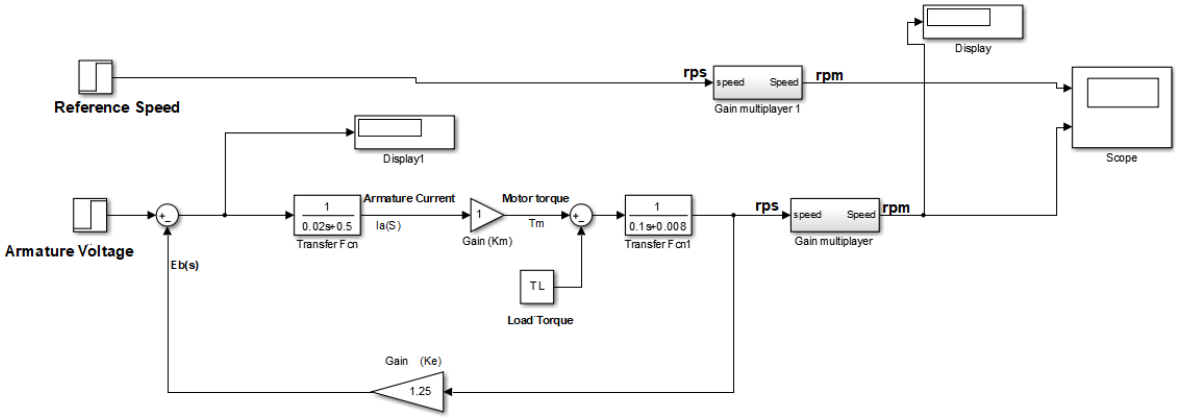

Figure 4.3: Block diagram of DC Motor without controller

4.1.1 Simulation of SEDCM Speed Control Without Controller at No Load

Figure 4.4 shows the Simulink model of SEDC Motor system. By applied 200 Volt input, Speed of the motor is 1509 rpm at no load (T_L=0).it has 9 steady state errors, settling time is 0.3180, rise time is 0.0674 and 14.28 overshoot.

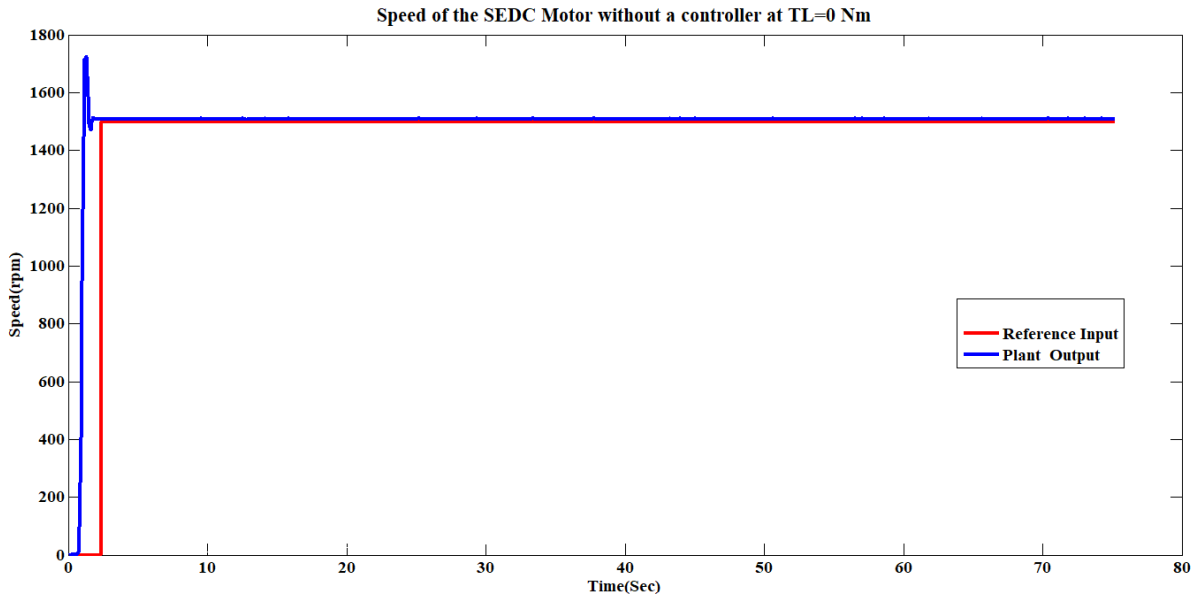

Figure 4.4: Speed of SEDC motor without a controller and at no load

4.1.2 Simulation of SEDCM Speed Control Without Controller at Half Load(TL=28.5 Nm)

Figure 4.5 shows the Simulink model of SEDC Motor system. Speed of the motor is 1401 rpm at half Load (T_L =28.5 Nm) it has 99 steady state errors, settling time is 0.3156, rise time is 0.0675 and 15.85 overshoot.

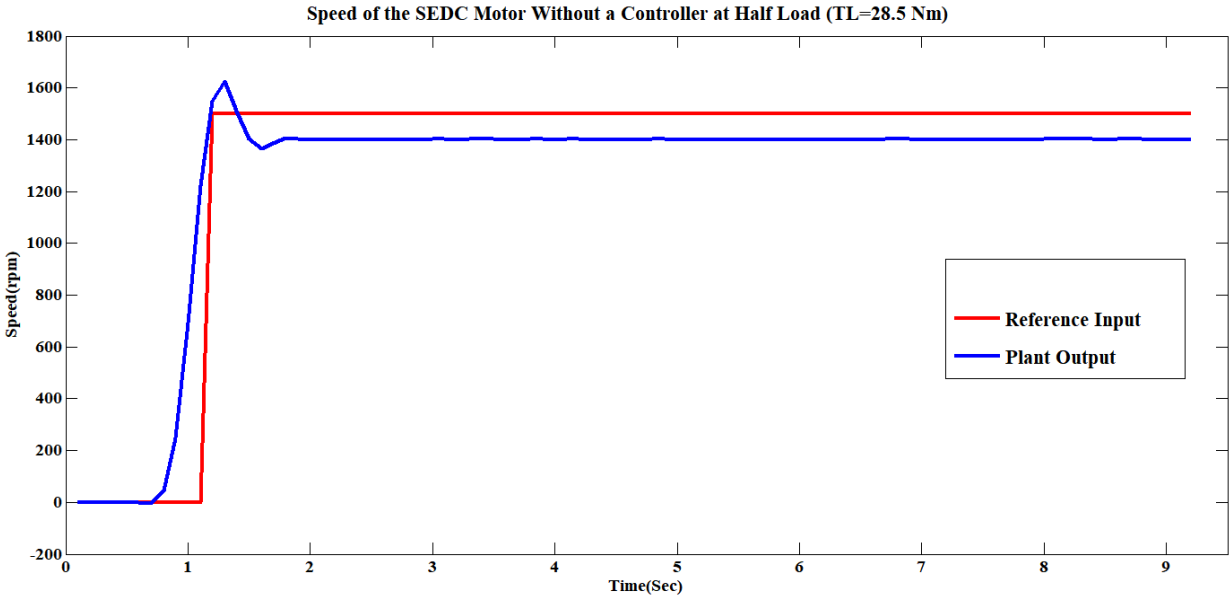

Figure 4.5: Speed of SEDC motor without a controller at Full Load(T_L =28.50 Nm)

4.1.3 Simulation of SEDCM Speed Control Without Controller at Full Load (TL=57 Nm)

Figure 4.6 shows the Simulink model of SED.C Motor system. Speed of the motor is 1294 rpm at Full Load (T_L =57 Nm).it has 206 steady state errors, settling time is 0.320, rise time is 0.0669 and 16.02 overshoot.

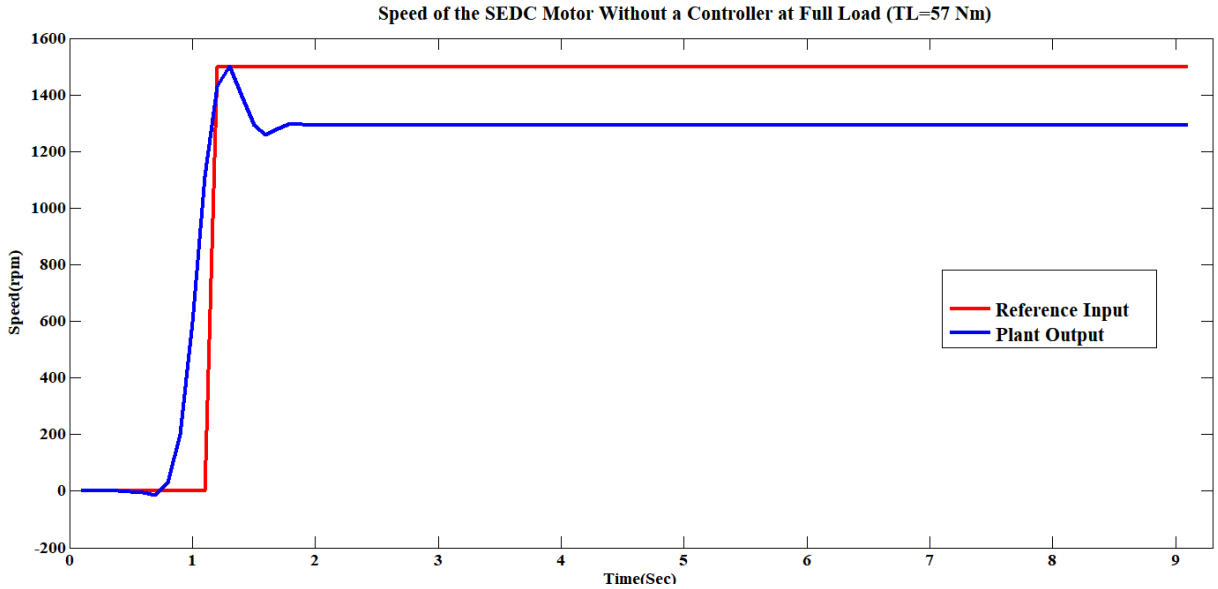

Figure 4.6: Speed of SEDC motor without a controller at Full Load (T_L =57 Nm)

4.1.4 Simulation of SEDCM Speed Control Without Controller at Different Load

Figure 4.7 shows The SEDC motor system's Simulink model. When the motor is powered by a 200-volt input, its speed is 1509 when there is no load (TL=0); when the load is increased to 28.5 Nm, the motor's speed decreases by 7.16 % to 108 rpm; the settling time increases by 0.0024 seconds, the steady state error increases by 99. When the torque load is increased to Full Load(TL=57 Nm), the motor's speed decreases by 7.63 % to 1294 rpm. Additionally, the steady state inaccuracy increases to 107 and the settling time increases by 0.004 seconds.

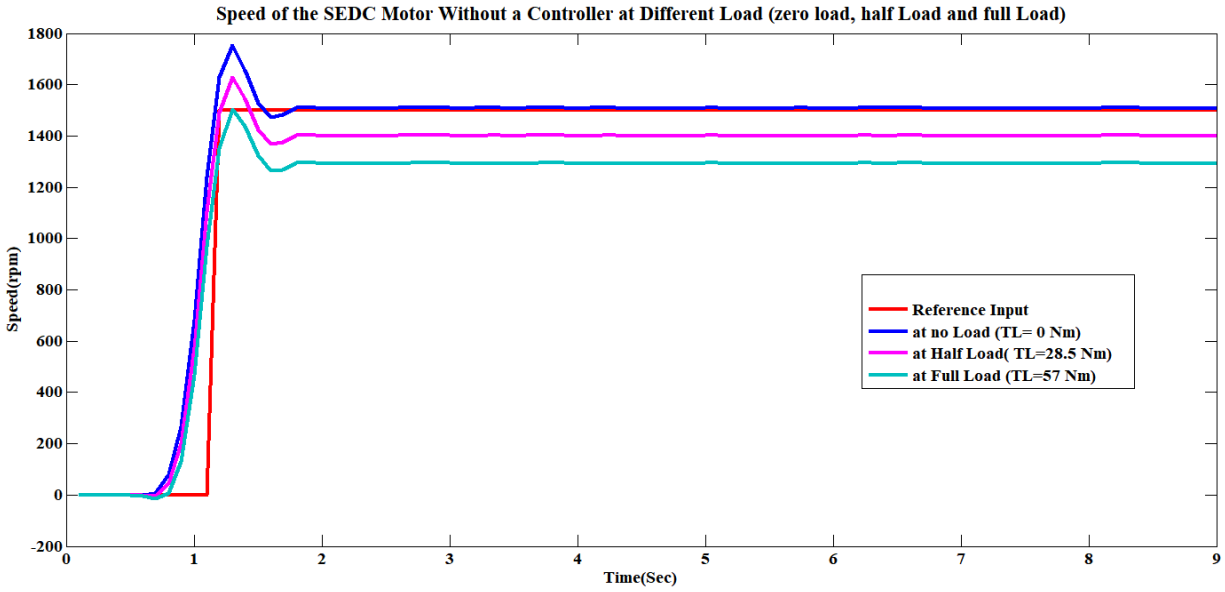

Figure 4.7: Speed of SEDC motor without controller at different load

Table-4.2: the performance of the motor at different load without controller

NO	Load(N m)	Speed Output (rpm)	t_r	t_s	Ess	Over shoot
1	At no load(T_L=0)	1509	0.0674	0.3156	9	14.28
2	At Half Load(T_L =28.5)	1401	0.0675	0.3180	99	15.85
3	At Full Load(T_L =57)	1294	0.0669	0.3200	206	16.02

4.2 Simulation of Speed Control of SEDC Motor Using PID Controller

The best gain value for Kp = 0.6(K_u)= 0.6*10.42= 6.252 , Ki = $\frac{1.2\,K_p}{T_u}$ = 7.502 , and Kd = $\frac{T_u * K_p}{8}$ = 0.7815 has been determined by Ziegler-Nichols tuning method. The optimal gain value combinations occur when the system can operate with the least amount of overshoot, steady state error, and steady state time. the PID controller's total simulation circuit. By applying 200 DC voltages to three distinct loads, I was able to quantify the motor's speed, steady state error (ess), rising time (t_r), settling time (t_s), and overshoot using a PID controller.

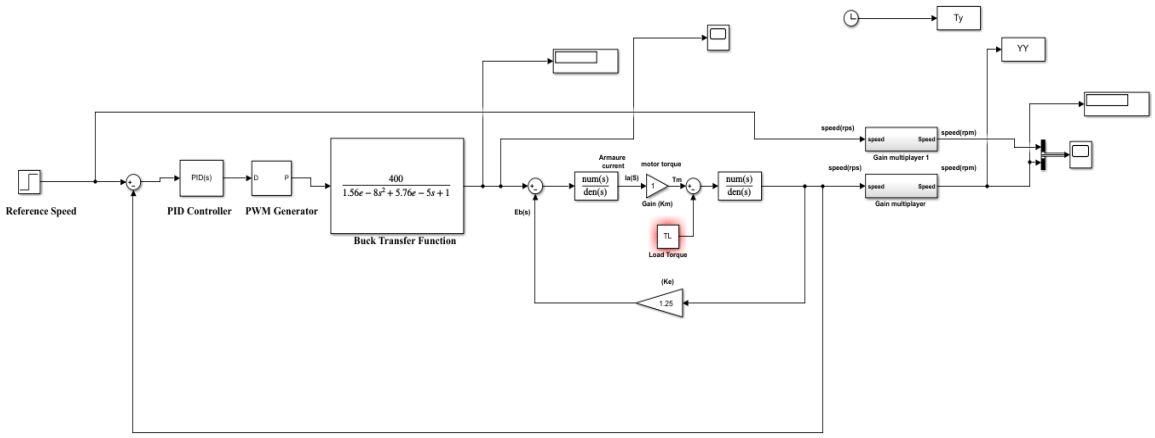

Figure 4.8: Block diagram of DC Motor Using PID controller

4.2.1 Simulation of SEDCM Speed Control Using PID Controller at No Load

Figure 4.9 shows the Simulink model of SEDC Motor with PID controller system. Speed of the motor is 1341 rpm at T_L =0 Nm.it has 159 steady state errors, settling time is 4.64, rise time is 2.51 and 23.78 overshoot.

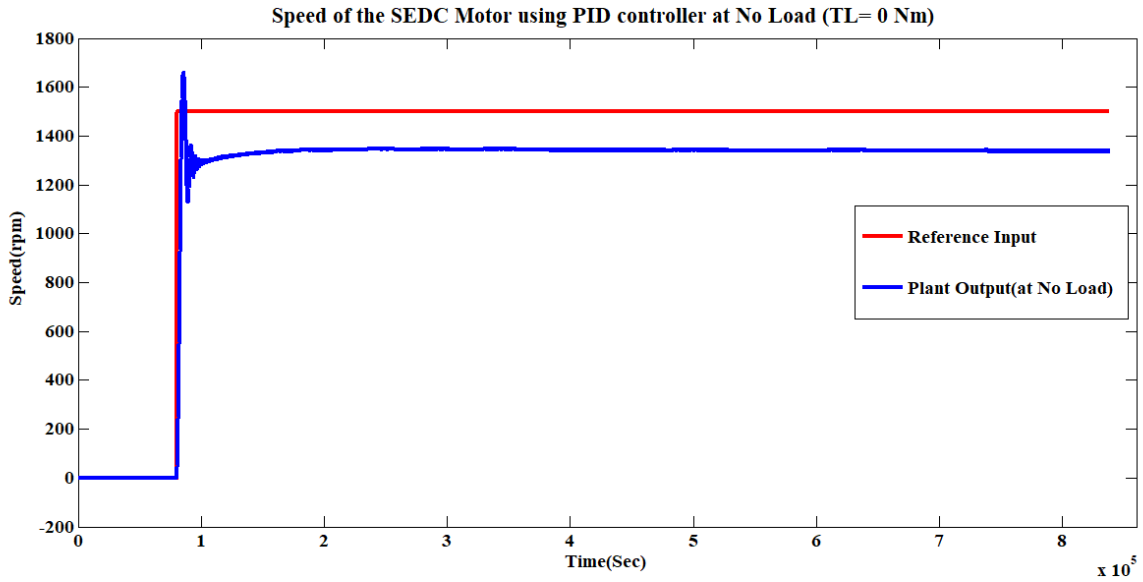

Figure 4.9: Speed of SEDC motor with PID controller and at no load (T_L =0 Nm)

4.2.2 Simulation of SEDCM Speed Control With PID Controller at Half Load(TL=28.5Nm)

Figure 4.10 shows the Simulink model of SEDC Motor with PID controller system. Speed of the motor is 1303 rpm at Half Load (T_L=28.5 Nm).it has 197 steady state errors, settling time is 11.56, rise time is 9.28 and 26.45 overshoot.

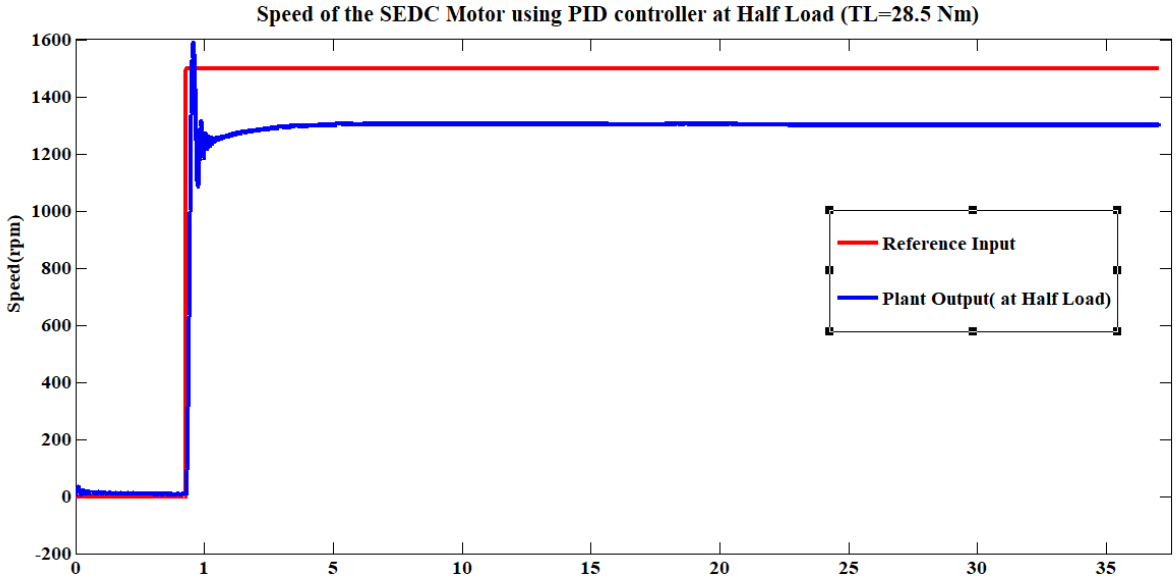

Figure 4.10: Speed of SEDC motor with controller at Half load (T_L =28.5 Nm)

4.2.3 Simulation of SEDCM Speed Control Using PID Controller at Full Load (TL=57 Nm)

Figure 4.11 shows the Simulink model of D.C Motor with PID controller system. Speed of the motor is 1284 rpm at Full Load (T_L =57 Nm).it has 216 steady state errors, settling time is 15.28, rise time is 11.84 Sec and 28.37 overshoot.

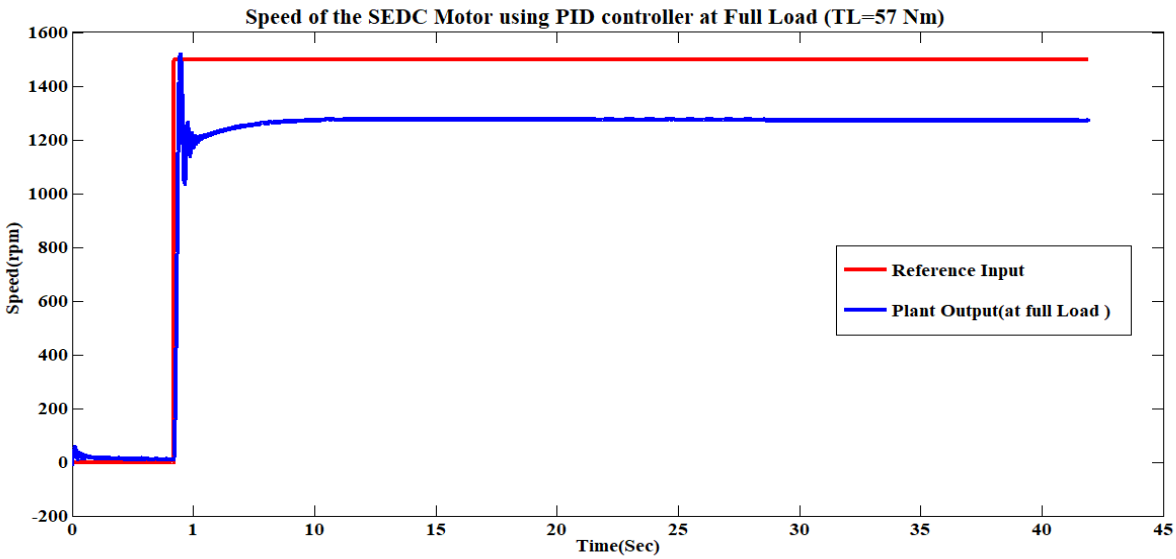

Figure 4.11: Speed of SEDC motor using PID controller at full Load (T_L =57 Nm)

4.2.4 Simulation of SEDCM Speed Control Using PID Controller at Different Load

Figure 4.12 shows the PID controller in the Simulink model of SEDC motor under various load conditions. the motor's speed at no load (TL=0) is 1341; when the load is increased to half Load (28.5 Nm), the motor's speed drops to 1303 rpm; the settling time increases by 7 seconds; and the steady state error increases by 38. When the torque load is increased from Half Load to full Load, the motor's speed drops to1284 rpm. The settling time also increases by 4 and rise time increase by 3 seconds and the steady state error increases by 19.

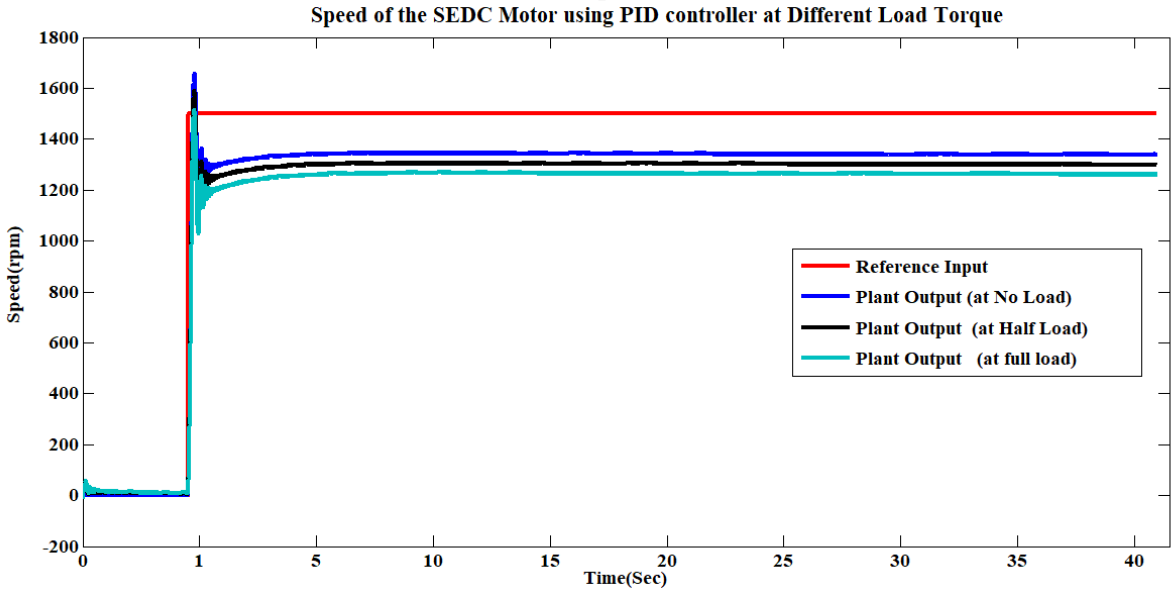

Figure 4.12: Speed of SEDC motor with PID controller and at different load

Table-4.3: the performance of the motor at different load with PID controller

NO	Load(N m)	Speed Output (rpm)	K_p	K_I	K_D	t_r(sec)	t_s	Ess	Over shoot
1	At no load(T_L=0)	1341	6.252	7.502	0.7812	2.51	4.64	159	21.90
2	At Half Load (T_L =28.5)	1303	6.252	7.502	0.7812	9.28	11.56	197	24.47
3	At Full Load(T_L =57)	1284	6.252	7.502	0.7812	11.84	15.28	216	28.37

4.3 Simulation of Speed control of SEDC Motor Using Fuzzy Logic Controller

The optimal gain value combinations occur when the system operates with little overshoot, minimal steady-state error, and minimal settling time. The comprehensive simulation circuit for the fuzzy logic controller. The fuzzy logic controller has been used to monitor the speed, steady-state error (ess), rising time (t_r), settling time (t_s), and overshoot of the motor under three distinct loads.

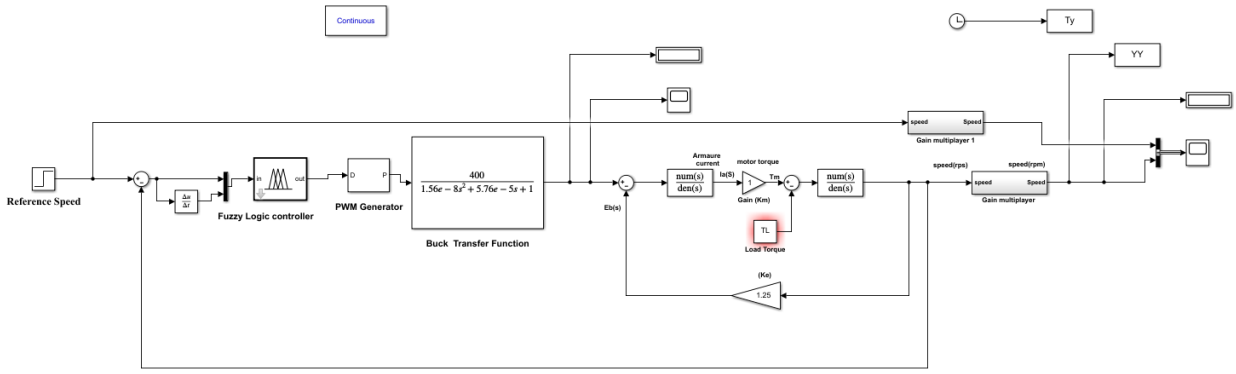

Figure 4.13: Block diagram of SEDC Motor with fuzzy logic controller

4.3.1 Simulation of SEDC Speed Control Using Fuzzy Controller at No Load

Figure 4.14: Shows the Simulink model of SEDC Motor with fuzzy logic controller system. Speed of the motor is 1484 rpm at no load (T_L =0 Nm).it has 16 steady state errors, settling time is 5.84, rise time is 4.73 and no over shoot.so we can observe from this less time response than without controller and PID controller.

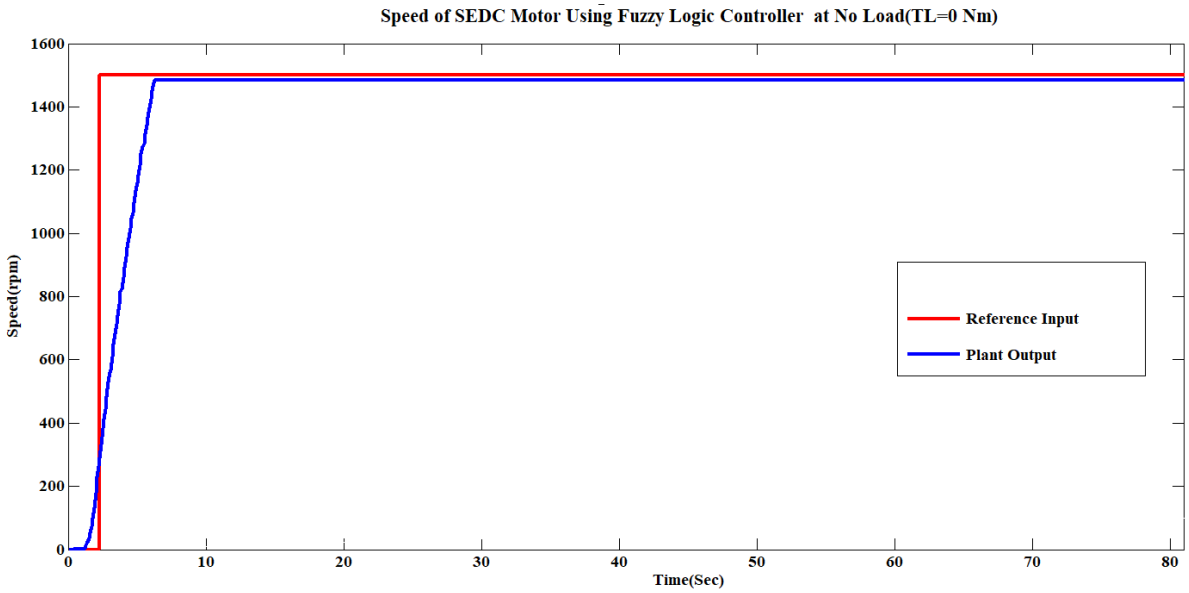

Figure 4.14: Speed of SEDC motor with fuzzy controller and at no load (T_L =0 Nm)

4.3.2 Simulation of SEDCM Speed Control Using Fuzzy Controller at Half Load

Figure 4.15 shows the Simulink model of SEDC Motor with fuzzy logic controller system. Speed of the motor is 1480 rpm at Half load(T_L =28.5 Nm).it has 20 steady state errors, settling time is 11.84, rise time is 9.28.

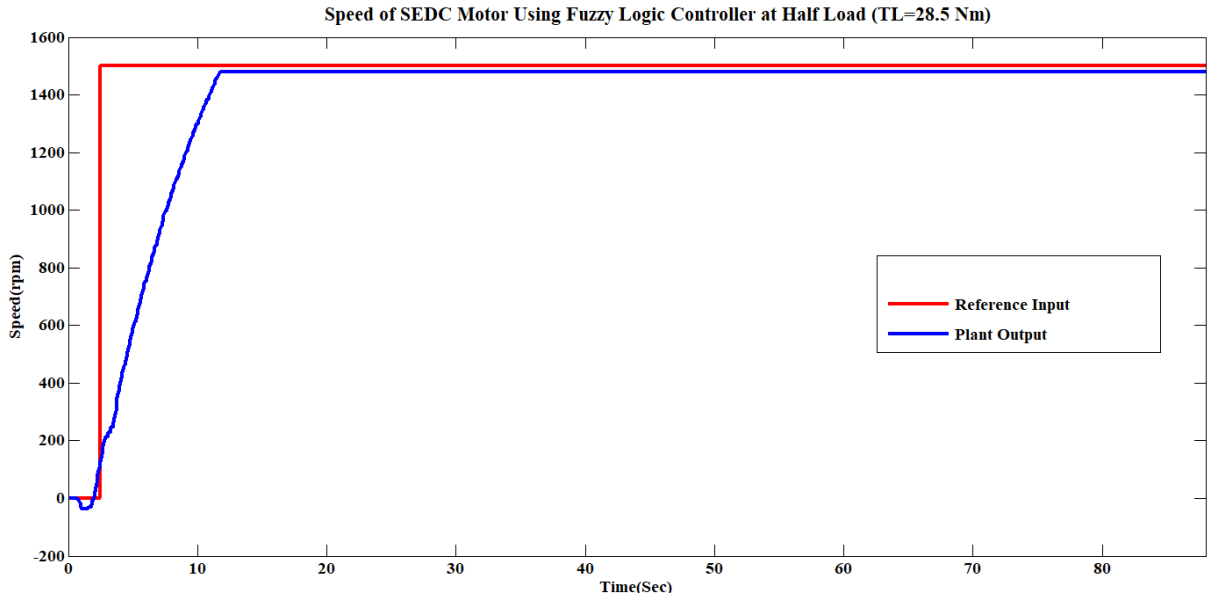

Figure 4.15: Speed of SEDC motor with fuzzy controller and at Half load (T_L =28.5 Nm)

4.3.3 Simulation of SEDC Speed Control Using Fuzzy Controller at Full Load (TL=57 Nm)

Figure 4.16 shows the Simulink model of SEDC Motor with fuzzy controller system.by applied 200 Volt input Speed of the motor is 1474 rpm at Full Load(T_L =57 Nm) it means the speed of DC motor will decrease as load torque increase.it has 26 steady state errors, settling time is 11.49 and rise time is 14.51. Then is less time response than without controller and PID controller.

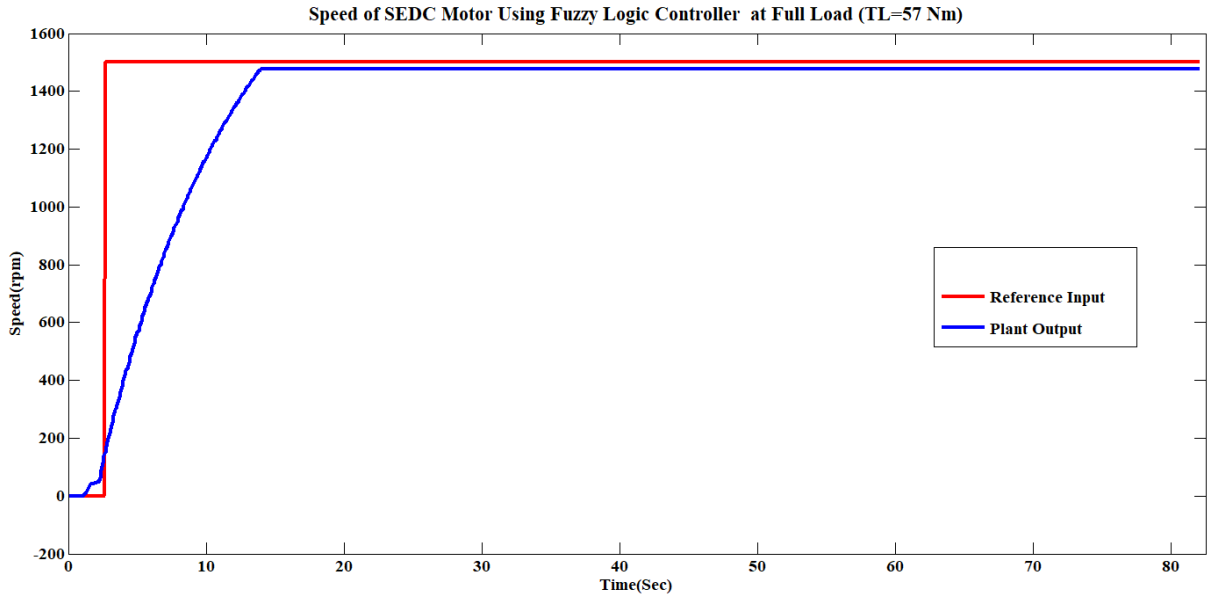

Figure 4.16: Speed of SEDC motor with fuzzy controller and at full Load (T_L =57 Nm)

4.3.4 Simulation of SEDCM Speed Control Using Fuzzy Controller at Different load

Figure 4.17 shows the SEDC motor Simulink model with fuzzy logic controller. the motor's speed is 1484 when there is no load (TL=0). When the load is increased to Half load, the motor's speed decreases by 4 Nm, its rising time increases by 4.55 seconds, and its settling time increases by about 6 seconds. The motor's speed decrease at a torque load increase to full load, reaching 1474 rpm. The settling and rising times increase by 2.67 and 2.21 seconds, respectively, and the steady state error is 26.

.

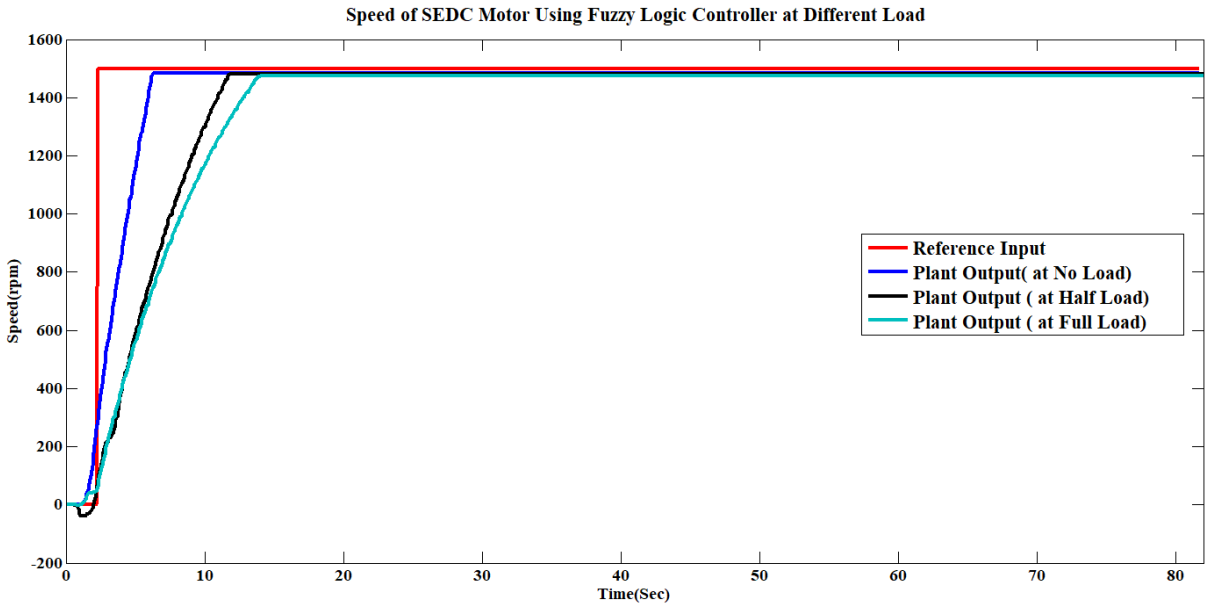

Figure 4.17: Speed of SEDC motor with fuzzy controller and at different load

Table-4.4: the performance of the motor at different load with fuzzy logic controller

NO	Load(N m)	Speed Output(rpm)	t_r(sec)	t_s(sec)	Ess	Over shoot
1	At no load(T_L=0)	1484	4.73	5.84	16	0
2	At Half Load (T_L =28.5)	1480	9.28	11.84	20	0
3	At Full Load(T_L =57)	1474	11.49	14.51	26	0

4.4 Simulation of Speed Control of SEDC Motor Using ANFIS Controller

The optimal gain value combinations occur when the system operates with minimal overshoot, minimal steady-state error, and minimal settling time. The comprehensive simulation circuit for the ANFIS controller. The speed, steady state error (ess), rising time (t_r), settling time (t_s), and overshoot of the motor's speed have been measured using ANFIS at three different loads with an applied voltage of 200 DC volts.

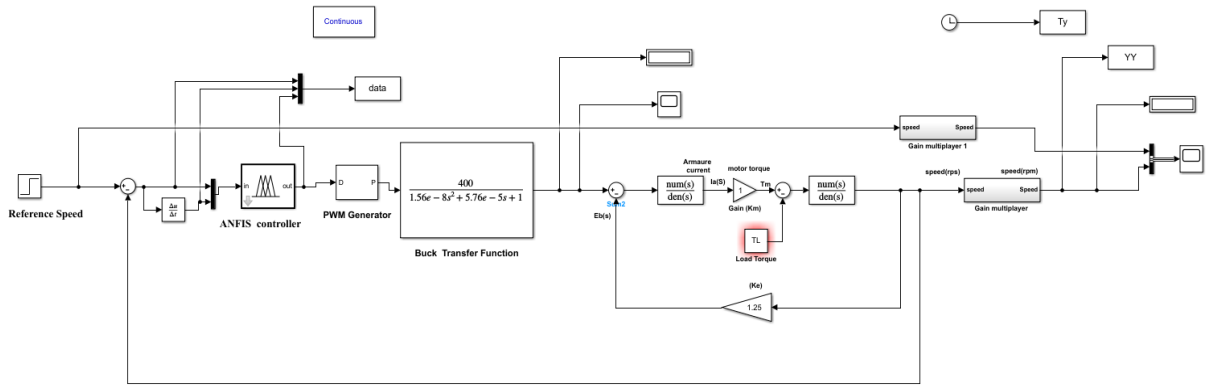

Figure 4.18: Block diagram of SEDC Motor Using ANFIS controller

4.4.1 Simulation of SEDC Speed Control Using ANFIS Controller at No Load

Figure 4.19 shows ANFIS controller system and SEDC motor Simulink model. At no load (TL = 0 Nm), the motor's speed is 1497 rpm. It has four steady state errors, no overshoot, a settling time of 2.95 and a rising time of 2.38. As a result, this time response is shorter than that of the PID and fuzzy logic controllers without controller.

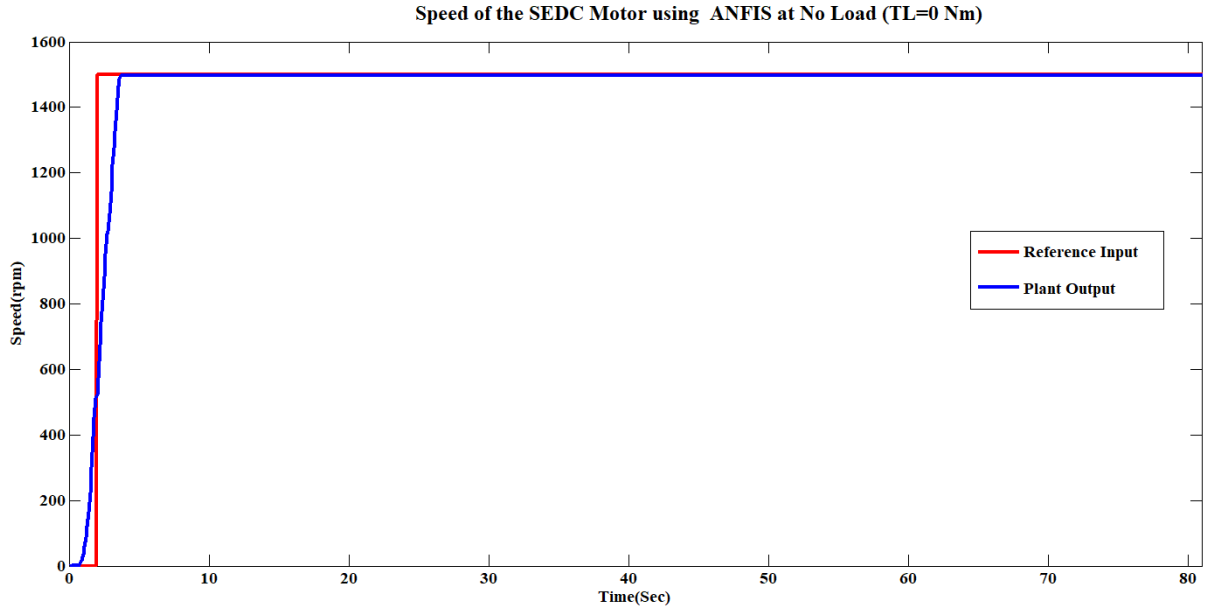

Figure 4.19: Speed of SEDC motor with ANFIS controller and at no load (T_L =0 Nm)

4.4.2 Simulation of SEDCM Speed Control Using ANFIS at Half Load (TL=28.5 Nm)

Figure 4.20 shows the Simulink model of SEDC Motor with ANFIS controller system. Speed of the motor is 1497 rpm at Half load(T_L =28.5 Nm).it has 3 steady state errors, settling time is 6.81 sec and rise time is 5.49 Sec.

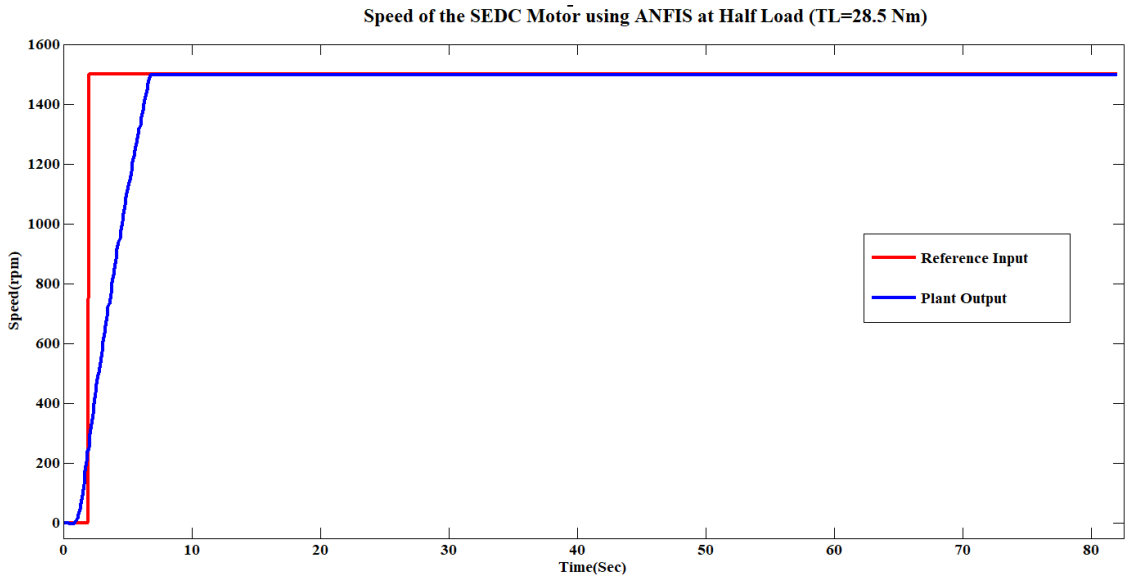

Figure 4.20: Speed of SEDC motor using ANFIS at Half Load (T_L =28.5 Nm)

4.4.3 Simulation of SEDCM Speed Control Using ANFIS at Full Load (TL=57 Nm)

Figure 4.21 shows the Simulink model of SEDC Motor with ANFIS controller system. Speed of the motor is 1497 rpm at Full load(T_L=57 Nm).it has 3 steady state errors, settling time is 10.11 sec and rise time is 7.92 Sec.

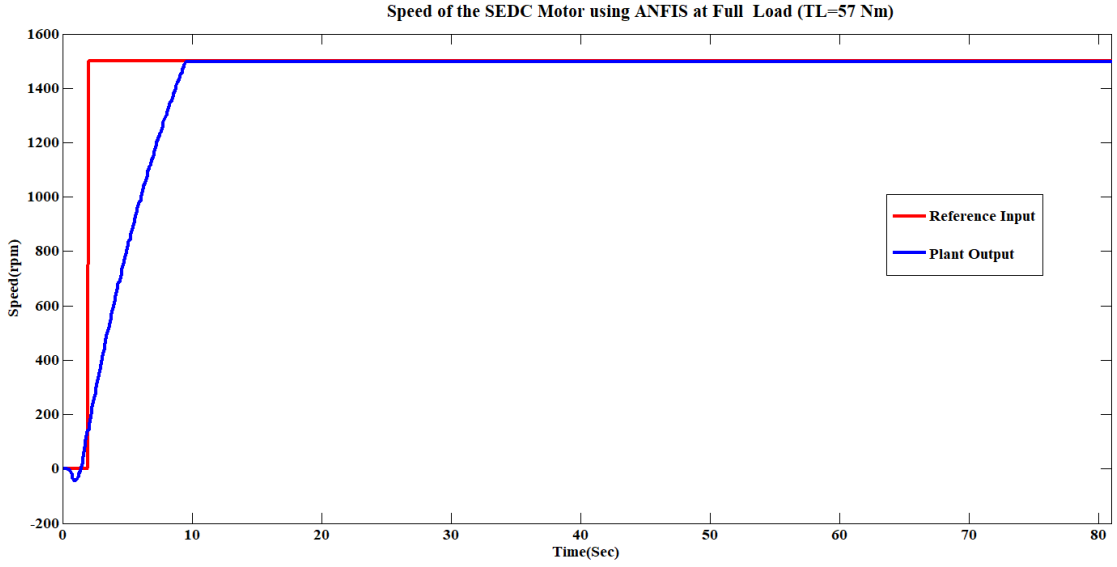

Figure 4.21: Speed of SEDC motor using ANFIS at Full load (T_L =57 Nm)

4.4.4 Simulation of SEDCM Speed Control Using ANFIS at Different Load

Figure 4.22 shows the Simulink model of the SEDC motor with ANFIS. When there is no load (TL=0), the motor runs at 1497 rpm. The motor's speed stays constant, its rising time increases by 3.11 seconds, and its settling time increases by around 3.8 seconds when the load is increased to

Half Load (28.5 Nm). At full load (57 Nm), the motor's speed stays constant, but the settling and rising times rise by 3.3 and 2.43 seconds, respectively.

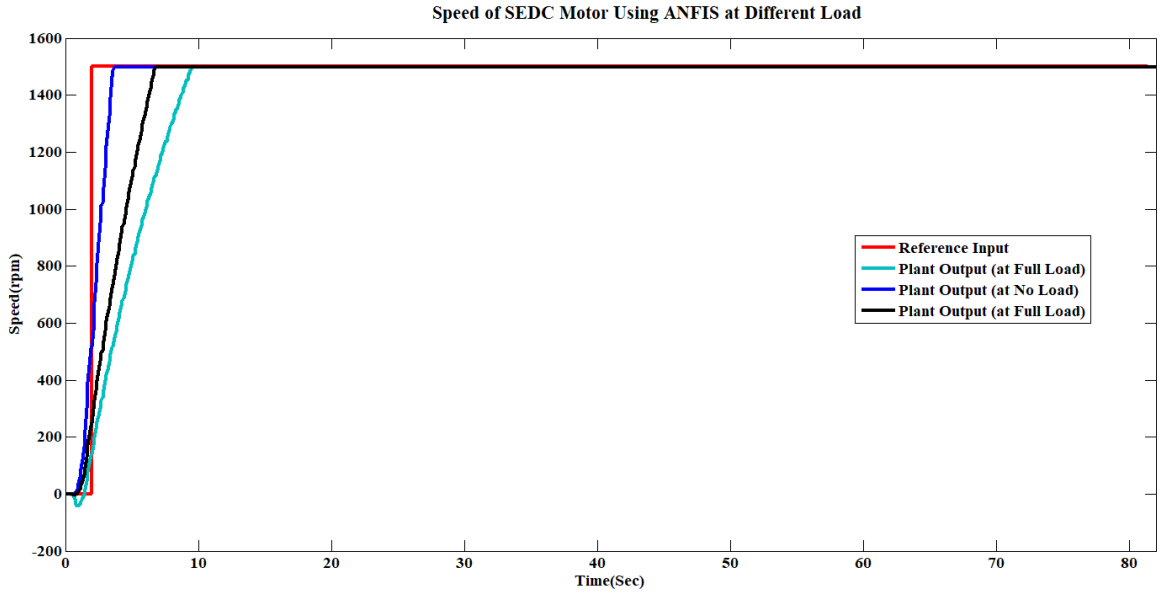

Figure 4.22: Speed of SEDC motor with ANFIS at different load

Table-4.5: the performance of the motor at different load with ANFIS

NO	Load(N m)	Speed Output(rpm)	t_r(sec)	t_s(sec)	Ess	Over shoot
1	At no load(T_L=0)	1497	2.38	2.95	3	0
2	At Half Load (T_L =28.5)	1497	5.49	6.81	3	0
3	At Full Load(T_L =57)	1497	7.92	10.11	3	0

4.4.5 Simulation of SEDCM input voltage from Duty cycle Using Different Controller

an Input Voltage (V_{in}), for a buck converter, V_{in} must be greater than V_0 , V_{in}= 400V for a good voltage difference, Duty Cycle (D) of buck converter is 0.5 and then the output voltage (V_0) will be 200 V.

Figure 4.23 shows the Input Voltage of the SEDC motor from Duty Cycle at Different controller like PID Controller, Fuzzy Logic Controller and ANFIS Controller.

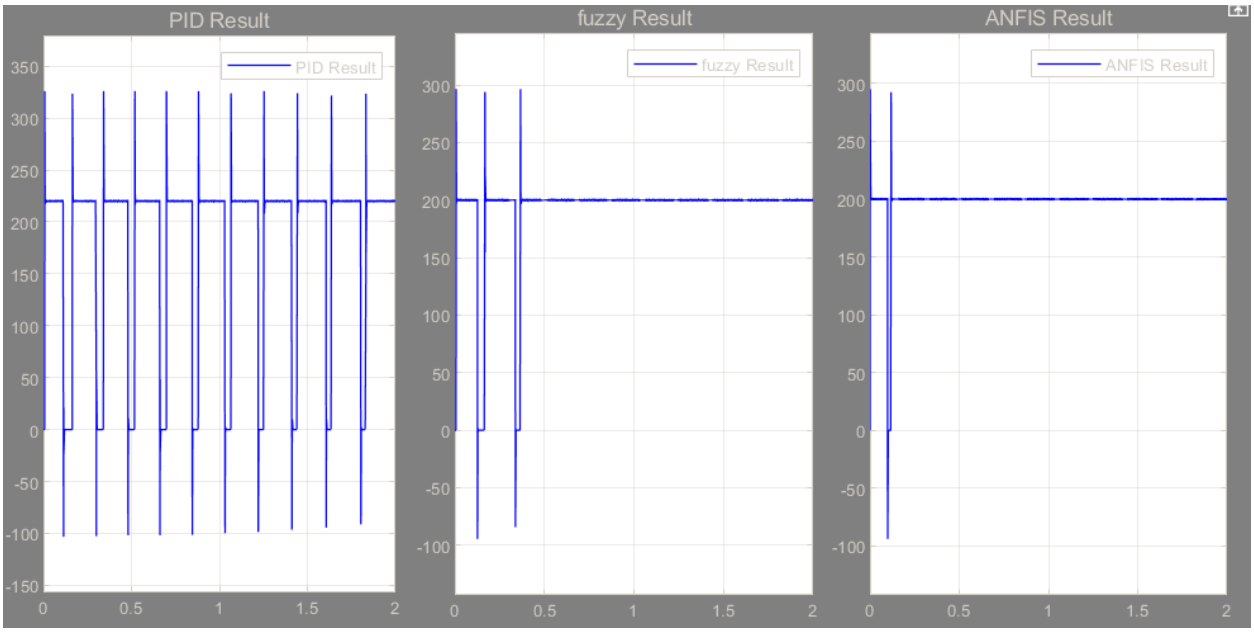

Figure 4.23: Input voltage of SEDC motor from Duty cycle at different controller

CHAPTER FIVE
CONCLUSION AND FUTURE WORK

5.1 Conclusion

ANFIS, fuzzy logic controllers, PID controllers, and open loop (without controller) have all been used to measure the speed of an independently stimulated DC motor. First, by altering the armature voltage, the motor's speed can be managed. One can regulate and change the motor's speed by altering the armature voltage(the source voltage). When the torque of the load grows and the transient and steady state faults rise, the motor's speed falls in the absence of a controller. The motor performs poorly as a result, and its speed will not maintain its rated level. A PID controller improves the motor's speed over an open loop, but the overall performance is still poor and there are still some transient and steady state issues. Although fuzzy logic controllers perform better than PID controllers in terms of system performance, the speed still fluctuates as the torque of the load changes. However, ANFIS better than fuzzy, PID, and open loop control systems, operates at its rated speed, has low steady state and transient errors, and keeps the motor's speed constant as the load increases.

In conclusion, NFIS is superior to fuzzy and PID controllers due to its zero overshoot and reduced 38.31% settling time compared to fuzzy and 50.93 % compared to PID, reduced 37.12% rise time compared to fuzzy and 44.87 % compared to PID, and reduced 85% steady-state error compared to fuzzy and 98.5 % compared to PID. Additionally, by resolving the motor's nonlinear properties, the system's overall performance will improve.

5.2 Future Work

As there is always a need to see a certain research topic using different approaches and methods, the following issue is recommended as future works:

- By considering external disturbance like Temperature, when the motor connected with other equipment, there is external characteristics that affect the motor performance then by solving those disturbance the speed of the motor will be better and high performance.
- Considering a separately excited DC motor connected to a load using a gearbox, belt and pulley system

References

[1]. W. I. Hameed and K. A. Mohamad, “Speed control of separately excited dc motor using fuzzy neural model reference controller,” *Int. J. Instrum. Control Syst. IJICS*, vol. 2, pp. 27–39, 2012.

[2]. P. Khanke and S. Jain, “Speed Control of Separately Excited DC Motor using various Conventional Controllers,” *Int J. Eng. Res. Appl.*, vol. 5, no. 4, pp. 67–72, 2015.

[3]. G. SHAHGHOLIAN and M. MAGHSOODI, “Analysis and Simulation of Speed Control in DC Motor Drive by Using Fuzzy Control Based on Model Reference Adaptive Control,” *Sci. J. CSJ*, vol. 37, 2016.

[4]. T.Venkatesh, M. Tarun kumar, B.Jayanthi, B. Ramesh, P. Chaitanya “Speed Control of DC Motor and Performance is Compared with PID and SMC Controller”volume6, issue no 4. ISSN 2321 3361 © 2016 IJESC, 10.4010/2016.

[5]. . Khoei, A. Hadidi, Kh, Microprocessor Based Closed-Loop Speed Control System For DC Motor Using Power MOSFET, Elctronics Circuits and Systems, IEEE International Conference ICECS 96, Vol. 2, 1247-1250, 1996.

[6]. Muhammad Rafay Khan, Aleem Ahmed Khan & Umer Ghazali, “Speed Control of DC Motor under Varying Load Using PID Controller”,International Journal of Engineering (IJE),Volume (9), Issue 3, 2015.

[7]. P. Khanke and S. Jain, “Speed Control of Separately Excited DC Motor using various Conventional Controllers,” *Int J. Eng. Res. Appl.*, vol. 5, no. 4, pp. 67–72, 2015.

[8]. A. T. Ali, E. B. M. Tayeb, and O. B. alzain Mohd, “Adaptive PID Controller for DC Motor Speed Control,” *Int. J. Eng. Invent.*, vol. 1, no. 5, 2012.

[9]. Rekha Kushwah and Sulochana Wadhwani , “Speed Control of Separately Excited DC Motor Using Fuzzy Logic Controller ”, International Journal of Engineering Trends and Technology (IJETT) – Volume:04, Issue:06, June 2013.

[10]. R.J. Wai, C.M. Lin, C.F. Hsu, "Adaptive Fuzzy Sliding Mode Control for Electrical Servo Drive", Fuzzy Sets and Systems, 143, 2004, pp.295-310.

[11]. A. Bernard, “Speed control of separately excited DC motor using artificial intelligent approach,” masters, Universiti Tun Hussein Onn Malaysia, 2013.
[12]. N. Pimkumwong and M.-S. Wang, “An Online Artificial Neural Network Speed Estimator for Sensorless Speed Control of Separately Excited DC Motor,” *2018 15th Int. Conf. Electr. Eng. Comput. Telecommun. Inf. Technol. ECTI-CON*, 2018, doi: 10.1109/ecticon.2018.8620021
[13]. S. C. Rajpoot, P. S. Rajpoot, Premlata, and D. Sharma, “Design and Simulation of Neuro Fuzzy Controller for Speed Control of a Separately Excited dc Motor,” *IOSR J. Electr. Electron. Eng. IOSR -JEEE*, vol. 11, no. 6, 2016.
[14]. J. Raheem Rashed, “Simulation of Speed Control for Separately Excited DC Motor Utilizing Fuzzy Logic Controller,” University of Thi-Qar Journal for Engineering Sciences, vol. 10, no. 1, pp. 141–146, Jun. 2019,
[15]. S. Bhowmik and A. Mitra, “Design of PID Controller for Separately Excited DC Motor and Its Performance Analysis,” International Conference on Energy, Systems, Drives, Power Electronics, Measurement and Sensors, Jun. 2023, Available:
[16]. R. Nagarajan, S. Sathishkumar, S. Deepika, G. Keerthana, J. K. Kiruthika, and R. Nandhini, “Implementation of Chopper Fed Speed Control of Separately Excited DC Motor Using PI Controller,” International Journal Of Engineering And Computer Science, Mar. 2017,
[17]. Dr.P.S. Bimbhra, “Electrical machinery”, Romesh Chander Khanna, Delhi, 7th ed, 2009
[18]. A. Sadiq, H. B. Mamman, and M. Ahmed, “Field Current Speed Control of Direct Current Motor using Fuzzy Logic Technique,” *Int. J. Inf. Comput. Technol.*, vol. 3, 2013
[19]. G. K. Mishra, A. K. Pandey, and A. Maurya, “Combined Armature and Field Speed Control of DC Motor for Efficiency Enhancement,” *SSRG Int. J. Electr. Electron. Eng. SSRG-IJEEE*, vol. 1, no. 6, Aug. 2014.
[20]. K. J. Astrom, B. Wittenmark, “Adaptive Control”, Lund Institute of Technology New York, 2nd ed, 2008.
[21]. Norman S Nice ,”Control Systems Engineering: , John Wiley and Son, USA, 4th ed, 2004
[22]. Chi-Tsong Chen “Analog and Digital System Design” state university of New York at stony brook pp. 556-557
[23]. A. F. M. S. Qadir, “Electro-Mechanical Modeling of Separately Excited DC Motor & Performance Improvement using different Industrial Controllers with Active Circuit Realization,” Khulna, BANGLADESH, 2014.

[24]. M. O. Okwu and O. Adetunji, “A comparative study of artificial neural network (ANN) and adaptive neuro-fuzzy inference system (ANFIS) models in distribution system with nondeterministic inputs,” Int. J. Eng. Bus. Manag., vol.10, pp.1–17, 2018, doi: 10.1177/1847979018768421.

[25]. Ronald S. Burns “Advanced control engineering” university of plymouth, UK, 1st ed, 2001

[26]. L. Zadeh and U. C. Berkeley, “Fuzzy Logic Guide Introduction of linguistic variables: Linguistic Rules,” 2003.

[27]. Roland S. Burns, “Advanced Control Engineering,” Butterworth-Heinemann, Jordan Hill, Oxford OX2 8DP, 2001.

[28]. A. Ghosh, “Hybrid Optimized Back Propagation Learning Algorithm for Multi-Layer Perceptron,” vol. 57, no. December, pp. 1–6, 2012.

[29]. U. Bansal and R. Narvey, “Speed Control of DC Motor Using Fuzzy PID Controller,” vol. 3, no. 9, pp. 1209–1220, 2013,

[30]. “Speed Control of Separated Excited DC Motor using Fuzzy Logic Controller,” *International Journal of Science and Research (IJSR)*, vol. 5, no. 5, pp. 2460–2464, May 2016, doi: https://doi.org/10.21275/v5i5.nov163971.

Appendix

Table A.1 specification of the DC Motor Parameters.

Descriptions of the parameter.	Parameter of value
Armature resistance (R_a)	0.5Ω
Armature inductance (L_a)	0.02 H
Armature voltage (V_a)	200 V
Mechanical inertia (J_M)	0.1 Kg.m2
Friction coefficient (B_M)	0.008 NM/rad/sec
Back emf constant (K_b)	1.25 V/rad/sec
Motor torque constant(K_t)	1 NM/A
Rated speed	1500 rpm
Rated power	12hp

B.Open loop modeling block of SEDC motor under different load torque

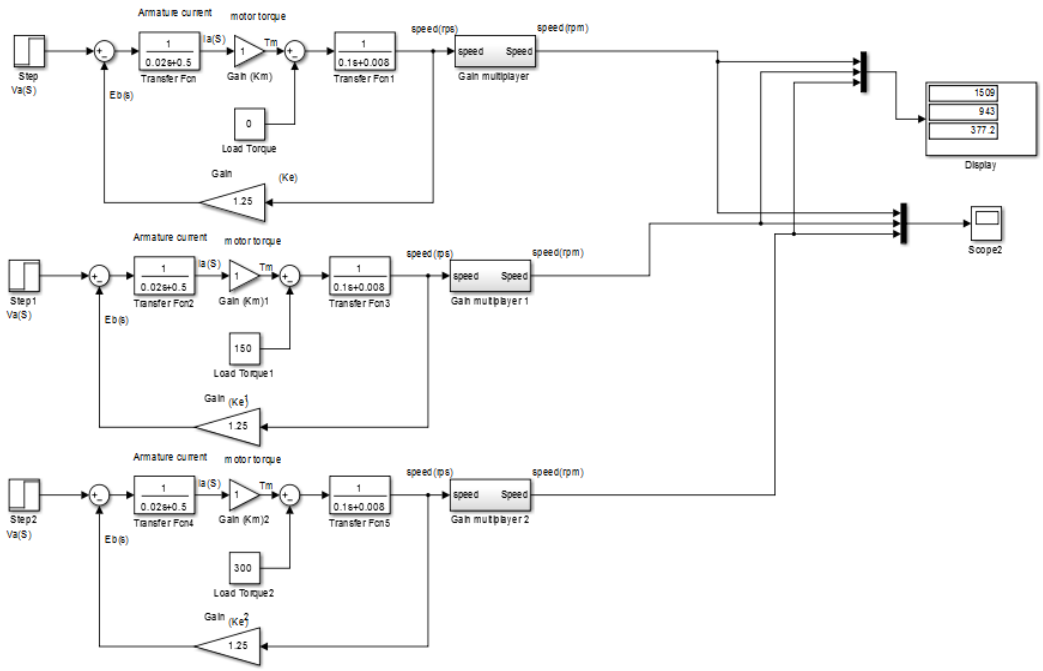

Fig B.1 Block diagram of DC Motor at open loop at different load

C. PID modeling block of SEDC motor under different load torque

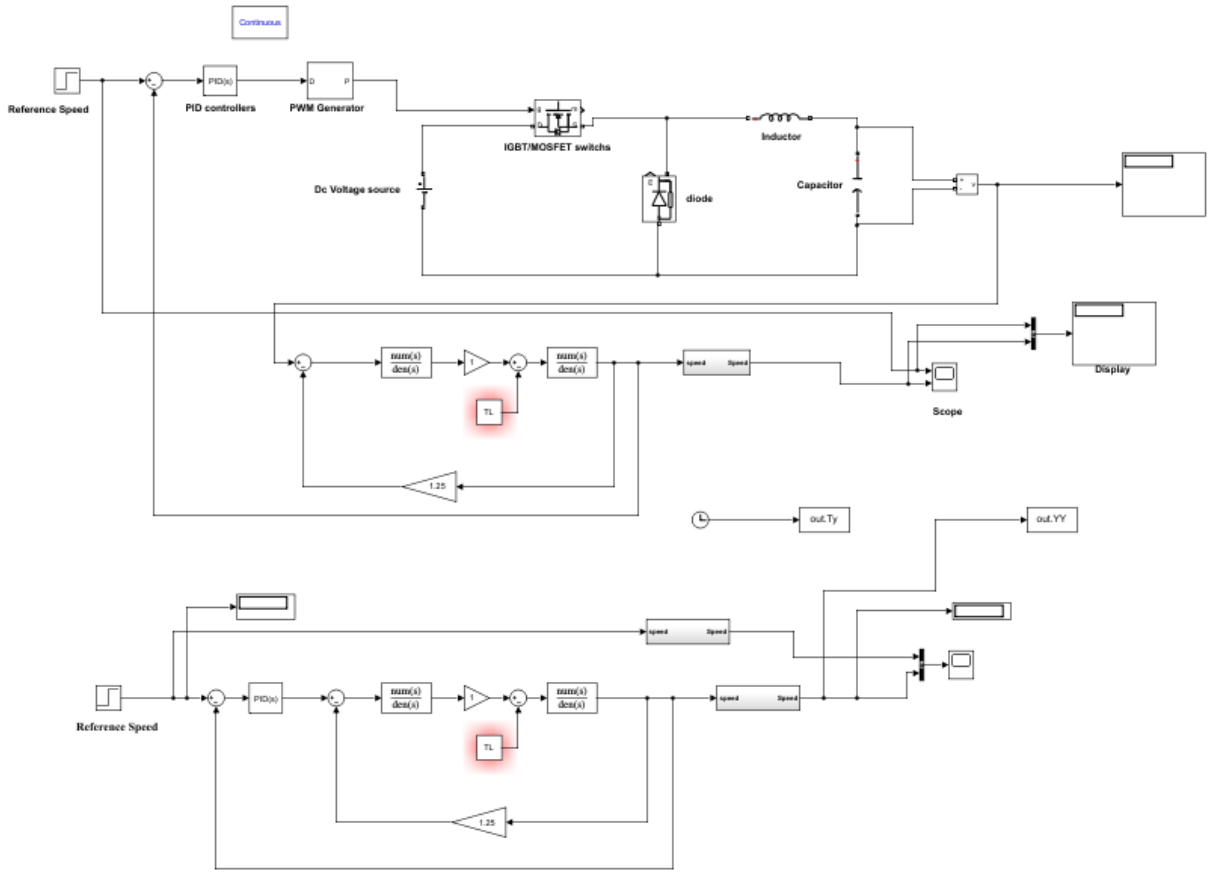

Fig C.1 Block diagram of SEDC Motor with PID controller at different load

D. Fuzzy logic modeling block of DC motor under different load torque

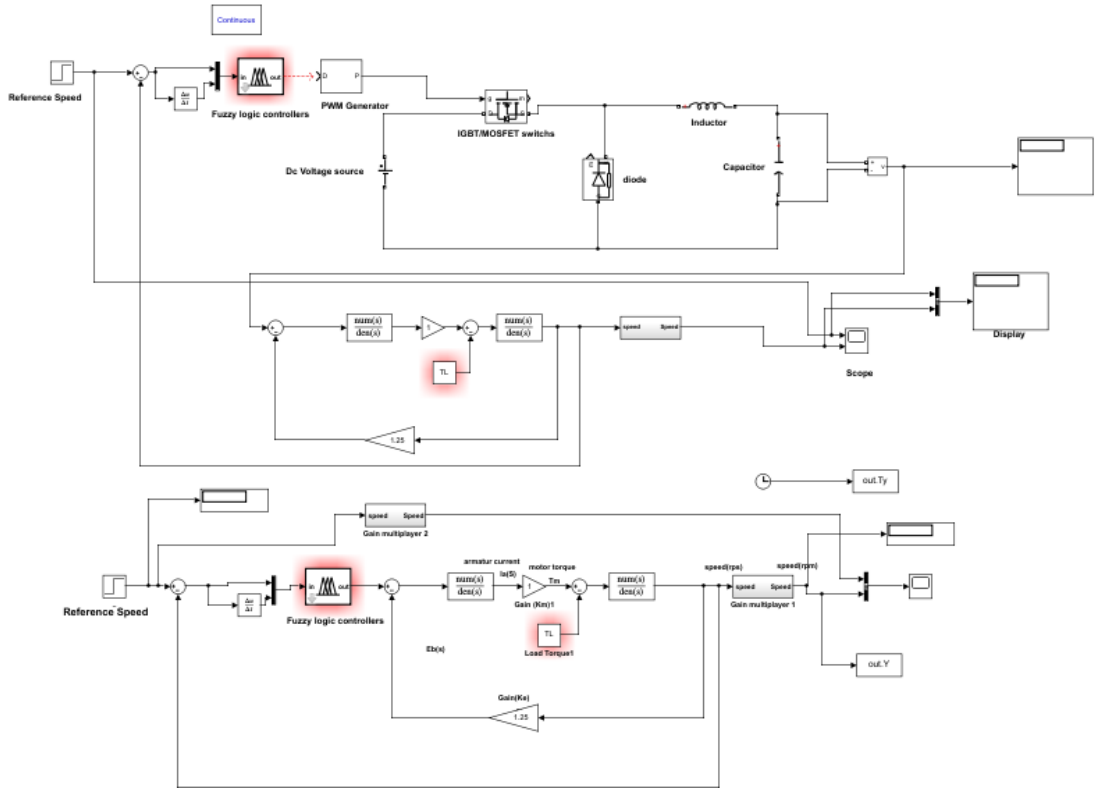

Fig C.1 Block diagram of SEDC Motor with with fuzzy controller at different load

E. ANFIS modeling block of SEDC motor under different load torque

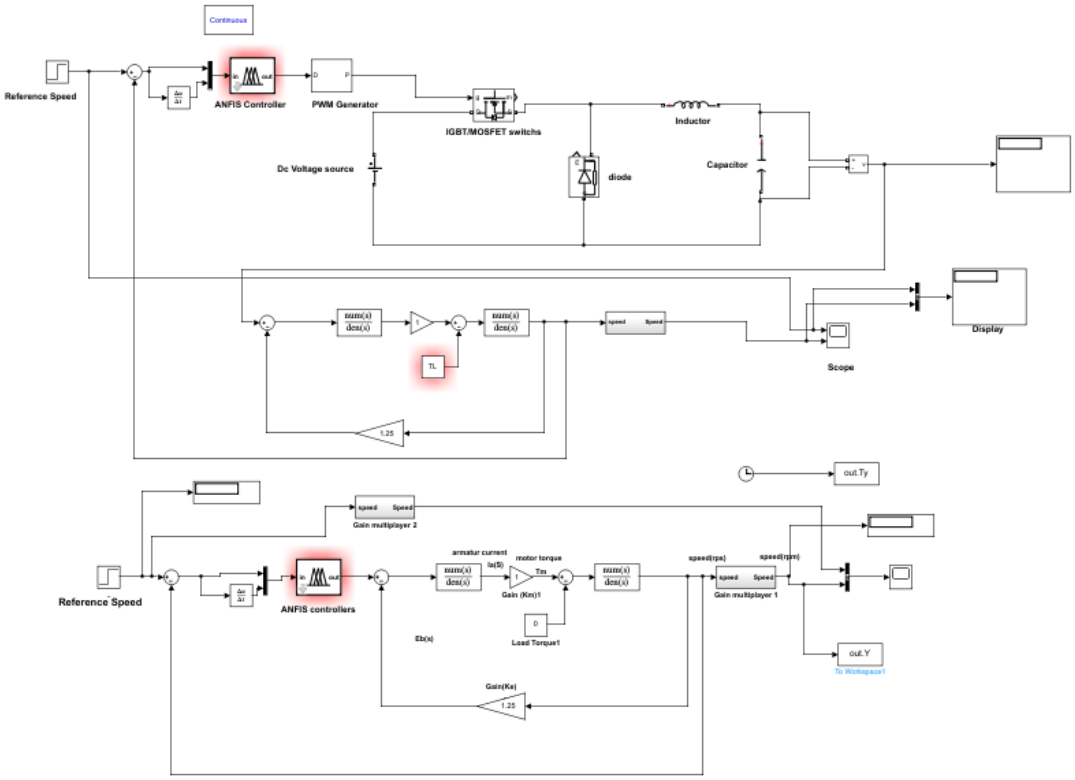

Fig E.1 Block diagram of SEDC Motor with with ANFIS at different load